Emekli-Alturfan Ebru (Orcid ID: 0000-0003-2419-8587)

Identification of Molecular Network of Gut-Brain Axis Associated with Neuroprotective Effects of PPARδ-Ligand Erucic Acid in Rotenone-Induced Parkinson's Disease Model in Zebrafish

İsmail Ünal[1], Derya Cansız[2], Mustafa Gani Sürmen[3], Saime Sürmen[3], Zehra Sezer[4], Merih Beler,[1] Ünsal Veli Üstündağ[2], Elif Güzel[4], A.Ata Alturfan[5], Ebru Emekli-Alturfan[6]

[1]Marmara University, Institute of Health Sciences, Faculty of Pharmacy, Department of Biochemistry, Istanbul, Turkey
[2]Department Medipol University, Faculty of Medicine, Medical Biochemistry, Istanbul, Turkey
[3]University of Health Sciences, Hamidiye Institute of Health Sciences, Department of Molecular Medicine, Istanbul, Turkey
[4]Department of Histology and Embryology, Istanbul University-Cerrahpasa, Cerrahpasa Faculty of Medicine, Istanbul, 34098, Turkey
[5] Istanbul University-Cerrahpaşa, Faculty of Medicine, Department of Biochemistry, Istanbul, Turkey
[6] Marmara University, Faculty of Dentistry, Department of Basic Medical Sciences, Istanbul, Turkey

Corresponding Author
Prof. Ebru Emekli-Alturfan (ORCID ID: 0000-0003-2419-8587)
Marmara University, Faculty of Dentistry,
Department of Basic Medical Sciences,
Istanbul, Turkey
ebruemekli@yahoo.com

Running Title: PPARδ-Ligand Erucic Acid and Parkinson's Disease

Data availability statement Data is available on reasonable request.

Consent to participate: All the authors have agreed for authorship, read and approved the manuscript, and given consent to participate.

Consent for publication: All the authors have agreed for authorship, read and approved the manuscript, and given consent for publication.

This article has been accepted for publication and undergone full peer review but has not been through the copyediting, typesetting, pagination and proofreading process which may lead to differences between this version and the Version of Record. Please cite this article as doi: 10.1002/ejn.15904

Funding statement: This work was supported by Marmara University Scientific Research and Project Commision Project No: TDK-2022-10377.

Declaration of competing interest: All authors declare that they have no competing interests.

Ethics approval statement: The experimental procedures were approved by the Institutional Animal Care and Use Committee of Marmara University (81.2021mar).

Abbreviation list

AChE: Acetylcholinesterase

AK: Adenylate kinase

ALP: Alkaline phosphatase

Cont: Control

DEP: Differentially expressed proteins

DMSO:Dimethyl sulfoxide

EA: Erucic Acid

ECM: Extracellular matrix

GO: Gene ontology

GST: Glutathione-S-transferase

LC-MS/MS: Liquid chromatography-mass spectrometry and tandem mass spectrometry

LPO:Lipid peroxidation

MDA: Malondialdehyde

NO:Nitric oxide

PD: Parkinson's disease

PPAR: Peroxisome proliferator-activated receptors

Rot:Rotenone

Rot+EA: Rotenone+Erucic Acid

RT PCR: Real Time Reverse transcription polymerase chain reaction

SOD: Superoxide dismutase

TH: Tyrosine hydroxylase

Abstract

Disruption of the gut-brain axis in Parkinson's disease (PD) may lead to motor symptoms and PD pathogenesis. Recently, the neuroprotective potential of different PPARδ-agonists has been shown. We aimed to reveal the effects of erucic acid, peroxisome proliferator-activated receptors (PPARs)-ligand in rotenone-induced PD model in zebrafish, focusing on the gut-brain axis. Adult zebrafish were exposed to rotenone and erucic acid for 30 days. LC-MS/MS analysis was performed. Raw files were analyzed by Proteome Discoverer 2.4 software, peptide lists were searched against *Danio rerio* proteins. STRING database was used for protein annotations or interactions. Lipid peroxidation (LPO), nitric oxide (No), alkaline phosphatase, superoxide dismutase, glutathione S-transferase (GST), acetylcholinesterase, and the expressions of PD-related genes were determined. Immunohistochemical tyrosine hydroxylase (TH) staining was performed. LC-MS/MS analyses allowed identification of over 2000 proteins in each sample. 2502 and 2707 proteins overlapped for intestine and brain. 196 and 243 significantly dysregulated proteins in the brain and intestines were found in rotenone groups. Erucic acid treatment corrected the changes in the expression of proteins associated with cytoskeletal organization, transport, and localization and improved locomotor activity, expressions of TH, PD-related genes (*lrrk2*, *park2*, *park7, pink1*), and oxidant-damage in brain and intestines in the rotenone group as evidenced by decreased LPO, No, and increased GST. Our results showed benefical effects of erucic acid as a PPARδ-ligand in neurotoxin-induced PD model in zebrafish. We believe our study, will shed light on the mechanism of the effects of PPARδ agonists and ω9-fatty acids in the gut-brain axis of PD.

Key words: Parkinson's disease, gut-brain axis, ω9-fatty acids, LC-MS/MS analyzes, zebrafish, rotenone

INTRODUCTION

Parkinson's disease (PD) is the second most common neurological disease disrupting the motor system. It is a chronic, progressive disease and the hallmarks of PD are cardinal motor impairment and synucleinopathy. The gut-brain axis has recently been discovered to be significantly influenced by the gut microbiome via immunological, neuroendocrine, and neurological mechanisms. Interestingly, in PD, disruption of the gut-microbiome-brain axis may lead to gastrointestinal symptoms, which may then impair the motor system and lead to PD pathogenesis (Dogra et al., 2022).

Protein accumulation, cell death with mitochondrial participation, and oxidative stress are all prevalent characteristics of neurodegenerative disorders, including PD. Patients are treated to alleviate symptoms, but the therapies do not address the underlying reasons, therefore the disease progresses unabated. In addition to known therapy options, it's intriguing to consider the role of diet in preventing the onset of the disease or slowing its course. Lipids or fatty acids have been suggested to avoid neurodegenerative illnesses. Various lipids can reduce cytotoxicity generated by disease, at the mitochondrial level, oxidative stress, apoptosis, or inflammation (Nury et al., 2020).

The nuclear receptor superfamily's peroxisome proliferator-activated receptors (PPARs) operate as ligand-regulated transcription factors that regulate gene expression in a variety of biological pathways (Tyagi et al., 2011). PPARα and PPARγ are expressed in different parts of the CNS, whereas PPARδ is the most widely expressed and is the most common subtype. Although there is limited evidence on the effects of PPARδ, studies have shown that PPARδ agonists provide neuroprotection following a variety of acute and chronic CNS traumas, including stroke, multiple sclerosis, and Alzheimer's disease. The neuroprotective potential of PPARδ agonists is assumed to be based on their antioxidant and anti-inflammatory characteristics (Schnegg and Robbins, 2011).

Kahremany et al. (2015) tested the computer modeling predictions against the experimental data available on different ligands and reported that erucic acid interacted well with the PPARδ

ligand binding domain (LBD). Erucic acid, a monounsaturated ω9-fatty acid (22:1ω9), is used as an edible oil in several Asian nations and by the Eskimos of Greenland. It's one of the ingredients in Lorenzo's oil, which is used to treat adrenoleukodystrophy (Nury et al., 2020). Erucic acid has been shown to exert an antioxidative activity that may overcome oxidative stress in neurodegenerative diseases (Altinoz and Ozpinar 2019). Accordingly, PPARδ and its ligand erucic acid have been suggested to prevent the progression of Parkinson's disease and the importance of examining the effect of erucic acid and PPARδ-activation in experimental animals has been suggested (Altinoz et al.,2021). However, the effects of erucic acid have not been reported in experimental models of PD so far.

In light of all this information, aim of our study is to reveal the effects of erucic acid in a rotenone-induced PD model in zebrafish, focusing on the gut-brain axis, by using proteomic, biochemical, immunohistochemical, gene expression, and behavioral analyses.

METHODS

Animals and treatment

Wild-type male/female zebrafish (8-10 months old) (AB/AB strain) were housed in a ZebTEC aquarium rack system (Tecniplast, Italy). Under a light/dark cycle of 14/10 h, zebrafish were kept in disease-free conditions at 27 ± 1 C. Animal experiments were carried out in accordance with the European Communities Council Directive of 24 November 1986 (86/609/EEC). The Institutional Animal Care and Use Committee of Marmara University approved all of the experimental procedures applied in this study. Fish were divided into four groups randomly and each group consisted of 15 fish. The control group included vehicle-treated healthy fish. Fish in the rotenone group (R) were exposed to 5 μg/l rotenone (Sigma, USA) which was dissolved in 0.1% dimethyl sulfoxide (DMSO) (Sigma, USA). The accumulation of lipid droplets in cardiac cells is the principal detrimental consequence of erucic acid in numerous animal species (Sissener et al., 2018). Unlike studies in warm-blooded species, there was no effect on weight increase in fish, presumably indicating that fish have a better tolerance for these fatty acids (Thomassen and Røsjø, 1989). In 2016, the European Food Safety Authority (EFSA) issued a risk evaluation of erucic acid, recommending a daily TDI of 7 mg kg^{-1} body weight for adults (EFSA, 2016). In our study, this dose was adapted to zebrafish and fish in the erucic acid group (EA) and rotenone+ erucic acid (ROT+EA) groups were gavaged every 3 days and 7 μl/g of erucic acid was given at once, at the same hour (between. 9:00 and 10:00 AM).

For the gavage procedure zebrafish were anesthetized by rapid cooling which was achieved within 10 s. After that fish were placed dorsal side up, into the groove in the sponge which was

previously soaked in the system water. The zebrafish's mouth was opened using the 22-G catheter tubing which was inserted gently into the esophagus until the tip was past the gills. The solutions containing erucic acid were injected slowly.

The water in the tanks of control and rotenone-treated groups was changed every 48 h to ensure constant uptake by the zebrafish. Zebrafish were fed commercial fish food (Tetramine) twice a day. Tetramine content is minimum 11% crude oil, 51% crude protein, 2.3% calcium, 1.5% phosphorus, maximum 15% ash, 3% crude fiber and 6.5% moisture. The granule size is 0.36–0.65 mm and its energy is 3.39 kcal / g. Amounts of rotenone was administered according to our previous studies (Unal et al., 2020; Yurtsever et al., 2020; Cansız et al., 2021).

At the end of 4 weeks, locomotor activities were determined and fish were anesthetized and euthanized by decapitation followed by rapid removal of the brain and intestinal tissues for RNA extraction and biochemical analysis. For the analysis of locomotor activity, biochemical parameters and RT PCR data analysts were blinded for the experimental condition.

Determination of behavior analysis

For the determination of locomotor activities, a rectangular transparent glass tank with dimensions (21 cm x 9 cm x 11 cm) and a volume (1.5 l) was used. Fish were transported in their housing tanks to the behavioral room and habituated to the environment for at least one hour before being transferred from their home tanks to the testing tank. The tests were performed between 1 pm and 4 pm. The water temperature and the lighting conditions of the tank were carefully matched to the home tank's water temperature and lighting conditions. The swimming pattern of each fish was recorded for 5 minutes by a camera mounted above the arena, which was used to start and monitor the experiment video. The camera was placed at a distance of 30 cm from the 21 cm long side of the tank. The water in the tank was changed to eliminate the potential effects of olfactory cues left by the prior fish.

The average speed and total distance traveled by the fish were analyzed using the Tox-Track program that detects and tracks animals inside closed arenas (Rodriguez et al., 2018). The exploration rate was also determined. A partition consisting of 25 frames on the y-axis and 60 frames on the x-axis was generated using the Tox-Track tracking software, and the ratio of zebrafish activity in vertical and horizontal areas of the tank were quantified and analyzed (Nadig et al., 2020).

LC-MS/MS proteomic analysis of brain and intestinal tissues

For proteomic analysis, 3 biological replicates were prepared for each group and three technical replicates were performed for each biological replicate. Extraction and digestion of the proteins

were performed according to the protocol we applied in our previous study (Sürmen et al., 2021), originally described by Wiśniewski et al (2009). In brief, 100 µg of protein extract was mixed with 8M urea and transferred to the filter device. After reducing with DTT 95˚C for 5 min, and alkylation with iodoacetamide at room temperature for 20 min, proteins were washed with urea and 50 mM ammonium bicarbonate, respectively. Then, proteins were digested with trypsin (enzyme-protein ratio: 1:100) at 37◦C for 18h. The obtained peptides were lyophilized and kept at −80 °C before use.

LC-MS/MS analysis was performed as described in our previous study (Sürmen et al., 2021). Three biological replicates in each group were analyzed at least three technical replicates. Peptide yields were resuspended in 0.1% FA and loaded onto a reverse phase trap column (Thermo Scientific Acclaim PepMap100, C18 5 µm× 0.3 mm, nano Viper C18) connected to the C18-reversed-phase analytical column (Thermo Scientific Acclaim PepMap100, C18, 2µm particle size, 75 µm diameter). The peptide mixture was separated with a gradient of mobile phase A (0.1% formic acid) and mobile phase B (0.1% formic acid in 85% acetonitrile) at a flow rate of 300nl/min controlled by Thermo Scientific Xcalibur software. The nanoLC system was coupled to a Q Exactive Plus Mass Spectrometer (Thermo Fisher Scientific) operated in the positive ion mode for data-dependent acquisition. Peptides were detected in survey scan from m/z 400-2000 with the Orbitrap resolution of 70 K (at 200 m/z).

The raw data obtained from MS were processed using Proteome Discoverer software (Version 2.3, Thermo Scientific). MS/MS spectra were searched against the reference proteome of *Danio rerio* available in UniProtKB database (UniProt Consortium, 2019) (containing 62031 sequences, downloaded on December 25, 2021) by Sequest search engine. For protein identification, the peptide validator filter false discovery rate (FDR) was set to 0.01, while the molecular weight of the precursor tolerance and the fragment tolerance could not exceed 10 ppm and 0.02 Da, respectively. *P* values for group comparison were calculated by the Proteome Discoverer platform, based on paired *t*-tests. Differentially expressed proteins were considered if proteins with a statistically significant abundance ratio of ≥ 2 (up-regulation, $p < 0.05$) or ≤ 0.5 (down-regulation, $p < 0.05$). After label-free protein quantitation, only proteins which were identified by two or more tryptic peptides were considered for further examination (with protein FDR ≤ 0.01).

InteractiVenn web-based tool was used to compare sets of data (Heberle et al., 2015). Protein interaction enrichment analysis was carried out using STRING 11.0 software (https://string-db.org/) and the network was visualized using Cytoscape program v3.8. The minimum required interaction score was set as 0.7 (high confidence) and disconnected nodes were hidden from

the network. Gene ontology (GO) terms were searched using the Cytoscape plugin BINGO tool (Maere et al., 2005). Fisher's Exact test was used to evaluate the enrichment analysis results, $p < 0.05$, followed by Benjamini−Hochberg False Discovery Rate correction.

Biochemical analyses

Brain and intestines were taken from anesthetized fish and, for each group tissues from four fish were pooled for each biological replicate, and for each biological replicate, three technical replicates were performed. Tissues were homogenized in physiological saline to prepare 10% (w/v) homogenates. After centrifuging briefly the supernatant was separated and used for the biochemical parameters. The method of Lowry (1951) was used to evaluate total protein levels and the results of the biochemical parameters were expressed per protein. Malondialdehyde (MDA) is a lipid peroxidation (LPO) end product and MDA levels were evaluated by using the method of Yagi (1984). The results of LPO were given as nmol MDA/mg protein. The levels of nitric oxide (NO) were determined by using the method of Miranda (2001) by reducing nitrate to nitrite using vanadium (III) chloride and the results were given as nmol NO/mg protein.

The activities of superoxide dismutase (SOD) were evaluated by using riboflavin-sensitized photo-oxidation reaction of o-dianisidine and results were given as U/mg protein (Mylorie et al.,1986). The activity of glutathione-S-transferase (GST) enzyme which catalyzes glutathione's conjugation was measured by spectrophotometer at 340 nm (Habig and Jacoby 1981). Acetylcholinesterase (AChE) activity and alkaline phosphatase levels were determined by the methods of Ellman (1961) and Walter and Schült (1974) respectively.

Reverse transcription (cDNA synthesis) and quantitative real-time PCR

For real-time PCR analysis, brain and intestinal tissues from three fish were pooled for each biological replicate for each group and, three technical replicates were performed for each biological replicate. Rneasy Mini Kit and Qiacube (Qiagen, Germany) were used to isolate RNA from each pooled brain and intestinal tissues. RT2 Profiler PCR Arrays (Qiagen, Germany) was used to synthesize single-stranded cDNA. DNA Master SYBR Green kit (Qiagen, Germany) was used for the PCRs. Qiagen Rotor Gene-Q Light Cycler instrument was used to determine the expression of PD-related genes *park2*, *park7*, *pink1* and *lrrk2*. Primer sequences are given in Table 1. Relative transcript levels were evaluated by using the Delta-Delta CT (DDCT) method through the normalization of the values to the housekeeping gene, β-actin (Livak and Schmittgen, 2001).

Immunohistochemical examination

To investigate the TH expression level in the dopaminergic neurons of the zebrafish brain, immunostaining of TH, a selected marker of dopaminergic neurons, was performed. Five zebrafish in each group (n=5) were used for IHC. The brain was fixed overnight in 2% paraformaldehyde (PFA) in 0.1 M phosphate buffer (pH 7.4) for up to 24 h at 4 °C. The brains were incubated in 25% sucrose solution (0.1 M phosphate buffer) for 2.5 hours and in 35% sucrose solution for 12 hours at 4°C until they sank. Then, the brains were embedded in sucrose (20 % w/v) – Gelatin (7.5% w/v, Sigma) horizontally and flash-frozen in liquid nitrogen. Serial sections (~5 µm) were taken using a cryostat, and IHC was applied blindly to 11th sections taken equally from each tissue. First of all, the slides were stored at −20 °C until further use. Brain sections were post-fixed in ice-cold 4% PFA (0.1 M phosphate buffer, pH 7.4) for 8 min at 4^{o}C. The tissue sections were blocked and incubated with mouse monoclonal anti-zebrafish Tyrosine Hydroxylase (TH) antibody (1:4000, #22941; Immunostar, Hudson, USA) for labeling dopaminergic cells overnight at 4^{o}C. For negative controls, antibody diluent (PBS) was used at the same concentration. The sections were washed three times for 5 min with TPBS (0.1% Tween) and then, biotinylated secondary antibody (SHP125; ScyTek, West Logan, Utah) was applied for 20 min. Afterward, streptavidin-peroxidase solution (SHP125; ScyTek, West Logan, Utah) was applied to the slides and 3,3′-Diaminobenzidine (DAB) (ACJ500; ScyTek, West Logan, Utah) was used as a chromogen. Subsequently, the sections were counterstained with Mayer's hematoxylin to label the nuclei. The sections were examined and photographed under Olympus BX61 digital microscope (Olympus, Tokyo, Japan) attached with a computerized digital camera and CellSens software (DP72; Olympus, Tokyo, Japan). The images of the diencephalon in each group were captured same adjustments and magnification. The diencephalon region in the zebrafish brain was determined according to Kaslin and Panula (2001) and Bartel et al. (2020). The dopaminergic neurons in the diencephalon region were evaluated, and the numbers of TH-positive cells in equivalent sections (11th) from each group were counted using Qupath software (Version 0.3.2; 2021) (Hein et al., 2021; Mysona et al., 2020; Bankhead et al., 2017). Positive cell detection was performed at the same threshold and adjustment.

Statistics

All statistical analyses were applied by using GraphPad Prism 9.0 (GraphPad Software, San Diego, USA) and the data were given as the mean ± standard deviation. The data was compared using one-way ANOVA test which was followed by Tukey's multiple comparison tests. The

data obtained were given as the mean ± standard deviation. p-value less than 0.05 was regarded as significant.

RESULTS

Results of locomotor activity

As rotenone is a mitochondrial complex 1 inhibitor that is known to increase ROS levels and cause a loss in dopaminergic neurons, we applied locomotor activity analyses to determine whether the movements of the fish were affected. Locomotor activities of the groups are given as average speed (A) and exploration rate (B) in **Figure 1.** The average speed and exploration rate of the rotenone group decreased significantly compared to the control group (ANOVA $F=5.31$, $df=1.195$, $p=0.005$, and ANOVA $F=8.26$, $df=0.147$, $p=0.0004$ respectively) ($p<0.05$ and $p<0.01$ respectively). Erucic acid treatment in the rotenone group improved both the average speed and exploration rate ($p<0.01$).

Results of LC-MS/MS proteomic analysis

Using the label-free proteomics approach with stringent filtering criteria, we identified a totally 4924 proteins in intestine tissue and 4386 proteins in the brain tissue of adult zebra fishes (Supplementary Table 1). Overall, our LC-MS/MS analyses allowed the identification of over 2000 proteins in each sample, with an average of around 2400 for all analyses. Protein identifications for each sample are given in Figure 2. The number of proteins matched with controls for each of the treatment groups is given in Figure 3.

Protein ratios from the control, rotenone, and erucic acid were calculated and statistical analyses revealed 196 significantly dysregulated proteins in rotenone-exposed zebrafish brain tissues. ($p < 0.05$, with at least two peptides). In the treatment groups shown with the Venn diagram in Figure 4A, the expression of 39 proteins from rotenone-induced DEPs significantly responded to Erucic acid treatment. In intestinal tissues, 35 of 243 DEPs were common with proteins altered by Erucic acid treatment ($p<0.05$), (Figure 4B). Details of differentially expressed these proteins are given in Tables 2 and 3. In addition, the altered abundances of these proteins detected in the control, rotenone and erucic acid treatment groups were shown by heatmap (Figure 5). With the heatmap, our aim was to show which of the proteins whose

expressions were changed by ROT responded to EA treatment and how similar the response was to the control group. The dendrogram nodes above the heatmap represent the similarity between the groups and accordingly the height of the nodes indicates that the control and EA groups were closer.

To understand the linkage of differentially expressed proteins and in what molecular processes they are associated, we performed a functional enrichment analysis. For GO analysis, 196 proteins in brain tissue and 243 in intestinal tissue whose expression changed after rotenone treatment compared to control were included. According to the GO analysis, rotenone affected proteins involved in calcium and lipid transport activity in brain tissues (Figure 6A). The top 5 categories of DEPs in intestinal tissues are phospholipase inhibitor activity, hydrolase activity, carboxypeptidase activity, cAMP-dependent protein kinase regulator activity, and lipid transporter activity in relation to protein phosphorylation, response to stimulus lipid transport, antigen processing, and presentation processes (Figure 6B). More information of p-values and FDR is given in Supplementary Table 3. Interestingly according to STRING enrichment results showed that proteins involved in metabolic pathways were highly represented ($p<0.001$), (Table 4).

Finally, we generated the interaction network of these proteins. As shown in Figure 7A, various hub proteins such as Eif3, Nhp2l1b, and Rps8 were associated with the spliceosome, RNA transport and translation in brain tissue. Moreover, in intestinal tissues, Atp5, which is important in oxidative phosphorylation, interacts with proteins that involved in energy metabolism. Ak1, Aco2, Ran, Mylpfa, and Mrpl13 are also among the proteins that interact with proteins and takes part in various cellular mechanisms. (Figure 7B).

In addition, Neflb, Si:dkey-33c12.3, Inab, Ckma, Rps8, Rps6, Mink1, Hmgb3a, Cst14b.1, Arl2, Ptmab, Marcksb, Tubb6, Viml, Aifm1, Anxa3b, Rnpep, Slc35a4, Ppp1r12a, Arl8ba, and Adh2.2 were among the treatment-responsive proteins in brain tissues, some of which highlighted the response to erucic acid treatment can be important to structural molecule activity, inhibitor activity and transporter activity (Figure 4A and 5A). We also observed that erucic acid treatment was effective on rotenone-induced DEPs in intestinal tissue (Figure 4B and 5B, Supplementary Table 2). These proteins were associated with electron transfer activity (Etfa, Etfb) oxidase activity (Cox6a1, Dao.2, Glrx), hydrolase activity (Gaa2, LOC100002544, Si:dkey-85k7.10, Si:ch211-201h21.5) antigen processing and presentation (Mhc1ufa, Mhc1uda, Si:busm1-266f07.1). However, erucic acid was not effective in reducing the expressions of Sumo3b (Ubiquitin conjugation pathway), Sqor (sulfide:quinone oxidoreductase, FAD binding), and Cpa5 (metallocarboxypeptidase activity, zinc ion binding)

sufficiently compared to the control group and also over-reduced the expression of Hpda (metal binding) and Vtg6 (lipid transporter activity) proteins (Figure 4B and 5B). We observed that erucic acid treatment mainly affected lipid metabolism in both brain and intestinal tissues exposed to rotenone.

Results of Biochemical Analysis

Oxidative stress plays a key role in the destruction of dopaminergic neurons in PD, leading to nitrative and oxidative damage to critical cellular components. To evaluate the oxidant/antioxidant status in the brain and intestines, levels of NO, lipid peroxidation (LPO) and activities of antioxidant enzymes superoxide dismutase (Sod) and glutathione S-transferase (Gst) were determined. Brain and intestinal LPO increased significantly in the rotenone groups groups (ANOVA F=365.6, df=0.52, p<0.0001; ANOVA F=39.02, df=0.66, <0.0001 respectively) (p<0.0001 and p<0.001 respectively) and erucic acid treatment decreased LPO significantly (p<0.0001 and p<0.001 respectively) (Figures 8A and 8B). Brain NO levels increased significantly in the rotenone group (p<0.0001) and erucic acid treatment decreased NO levels significantly in both brain and intestinal tissues (ANOVA F=54.87, df=1.121, p<0.0001; ANOVA F=27.03, df=0.79, p=0.0002 respectively) (p<0.01) (Figure 8C and 8D).

Superoxide dismutase (Sod) is an antioxidant enzyme that converts superoxide to H_2O_2 (Saravanan et al., 2006). In our study, brain Sod activities increased (p<0.001) whereas intestinal Sod activities decreased significantly in the rotenone group (ANOVA F=41.26, df=0.98, p<0.0001; ANOVA F=61.06, df=0.99, p=0.0002 respectively) (p<0.001). Erucic acid treatment in the rotenone group increased brain Sod activities (p<0.01) but decreased intestinal Sod activities (p<0.05) compared to the rotenone group (Figures 9A and 9B).

As phase-II detoxification enzymes GSTs have a cytoprotective role by catalyzing the conjugation of reduced glutathione (GSH) with reactive electrophiles (Ozdamar and Can-Eke, 2013). To evaluate the effect of erucic acid on detoxification metabolism in the case of rotenone toxicity Gst activities in the brain and intestines were determined. Both brain and intestinal glutathione S-transferase (Gst) activities increased significantly in the erucic acid-treated fish (ANOVA F=147.1, df=0.28, p<0.0001; ANOVA F=79.95, df=0.31, p<0.0001respectively) (p<0.01 and p<0.001 respectively) and decreased significantly in the rotenone groups when compared to the control group (p<0.05 and p<0.01 respectively). Erucic acid treatment in the rotenone groups increased Gst activities significantly in the brain (p<0.0001) and intestines (p<0.05) (Figures 9C and 9D).

AChE is necessary for the maintenance of balanced cholinergic and dopaminergic systems, for appropriate basal ganglia function (Zhou et al., 2003). In our study, erucic acid treatment led to a significant increase in intestinal AChE activity (ANOVA F=16.65, df=1.02, p=0.0008) ($p<0.01$). Brain AChE activity decreased in the rotenone group (ANOVA F=3.75, df=0.55) ($p<0.05$) but no change was observed in the intestinal AChE activity of the rotenone group. Intestinal AChE activity increased significantly in the erucic acid-treated rotenone group when compared with the rotenone group ($p<0.05$) (Figures 10A and 10B). Brain alkaline phosphatase (Alp) levels increased ($p<0.05$) whereas intestinal Alp levels decreased significantly ($p<0.01$) in the erucic acid treated group (ANOVA F=54.97, df=0.13, $p<0.0001$; ANOVA F=16.65, df=1.02, p=0.0008 respectively). Rotenone treatments led to significant decreases in both brain and intestinal Alp levels ($p<0.001$ and $p<0.0001$ respectively). Erucic acid treatments in rotenone groups increased Alp levels in both brain and intestines ($p<0.0001$ and $p<0.05$ respectively) (Figure 10C and 10D).

Results of Gene Expression Analysis

The expressions *park2, park7, pink1,* and *lrrk2* were determined as they are associated with mitochondrial functions in PD. Park2 facilitates mitochondrial maintenance under physiological conditions (Weihofen et al., 2009) and it may cause defective mitochondria to undergo autophagy (Narendra et al., 2008). The Pink1 is a serine/threonine kinase that is thought to play a role in the mitochondrial response to cellular and oxidative stress (Valente et al., 2004). It is also a key component of the Pink1/parkin pathway, which regulates mitochondrial morphology and function in response to stress (Nuytemans et al., 2010). Park7 (Dj-1) is H_2O_2-responsive, implying that it functions as an antioxidant and serves as a sensor for oxidative stress (Zhang et al., 2005). Park7, park2, and Pink1 have been suggested to be part of a new E3 ligase complex (Xiong et al., 2009).Lrrk2 is involved in many different cellular processes to initiate mitophagy in a PINK1/parkin-dependent manner (Wauters et al., 2020). We found significantly increased expressions of brain *lrrk2, park2, park7* and *pink1* in the erucic acid group compared to the control group (ANOVA F=638, df=3.61, $p<0.0001$; ANOVA F=224, df=0.82, $p<0.0001$; (ANOVA F=575.4, df=3.11, $p<0.0001$; ANOVA F=141.6, df=2.51, $p<0.0001$respectively) ($p<0.05$, $p<0.01$, $p<0.05$ and $p<0.05$ respectively); however, the most significant increases were observed in the rotenone groups ($p<0.0001$). Erucic acid treatment in the rotenone group decreased the expressions of *lrrk2, park7,* and *pink1* ($p<0.0001$) but increased the expression of *park2* ($p<0.01$) (Figure 11).

Results of Tyrosine Hydroxylase (TH) immunostaining

TH catalyzes the formation of L-DOPA which is the rate-limiting step in dopamine biosynthesis. This enzyme may thus play a role in the development of PD on multiple levels, as well as being a prospective candidate for generating new treatments for the disease (Haavik and Toska,1998). TH immunostained cells in the diencephalon region were evaluated to determine the effect of erucic acid in the rotenone induced PD in zebrafish (Figure 12). There was no statistically significant difference between the control and erucic acid groups. TH-positive cells significantly decreased in the rotenone group compared to the control group (Figures 12A and 12C). Rotenone considerably reduced the number of dopaminergic neurons compared to the control group in the diencephalon of the zebrafish brain (Figure 12F). The number of dopaminergic neurons significantly increased in the rotenone+erucic acid group compared to the rotenone group (ANOVA $F=232.4$, $df=0.47$, $p<0.0001$) (Figures 12A,12D, and 12F). There was a statistically significant difference between erucic acid and rotenone+erucic acid groups (Figures 12B,12D, and 12F).

DISCUSSION

PD is an insidious illness that affects 1-2 percent of the population over 65 years old. Understanding the cause of PD might lead to the development of novel therapies. Although genomic and transcriptome investigations are beneficial, they do not give proof of the disease's current condition. Proteomic investigations, on the other hand, deal with proteins that are real-time participants and may thus give insight into the dynamic character of the afflicted cells (Kasap et al., 2017). Therefore, in our study, we investigated the effects of erucic acid as a PPARδ ligand, on the experimental PD model, using proteomic methods and analyzing the expressions of molecules and genes associated with mitochondrial functions.

Qualitative and quantitative proteomic studies showed mitochondrial dysfunction as one of the main metabolic events in PD (Kasap et al., 2017). In our study, we used proteomic methods to determine through which pathways and which proteins erucic acid exerts its possible effects in the brain and gut in the experimental PD model. Results of the proteomic analysis showed significantly dysregulated proteins both in the intestines and brain tissues of rotenone-exposed zebrafish. Splicing factor proline and glutamine-rich (SFPQ), RNA-DNA binding protein, has been shown to be dysregulated in Alzheimer's disease frontotemporal dementia and suggested to be a pathological characteristic of the CNS of ALS patients (Hogan et al., 2021). According to our proteomic analysis results, we observed decreased expression of intestinal SFPQ in the rotenone-treated group. Paraspeckles are defined as the foci containing NEAT1_2 and an essential RNA-binding paraspeckle protein such as SFPQ (Fox, 2018). According to a recently

discovered mitochondria-paraspeckle interplay, paraspeckle abundance is controlled by a wide collection of nucleus-encoded genes that regulate mitochondrial activities and the absence of paraspeckles is reported to be sufficient to produce mitochondrial abnormalities, such as decreased respiration and ATP generation, as well as faulty mitochondrial fission (Wang 2018). The effects of mitochondrial stress on paraspeckles have been shown to be mediated in part by damaged mitochondria inducing an immunological response (An et al., 2018). In our study, rotenone exposure decreased intestinal SFPQ but no change was observed in the brain which may be associated with decreased intestinal paraspeckles, supporting the view that disturbances of the mechanisms regulating intestinal functions may be among early events of PD.

We used Venn diagram to identify the molecular functions and biological processes of rotenone-induced DEPs that responded to erucic acid treatment and in the brain they were found to include mainly substrate-spesicific transporter activity, structural molecule activity, and organization of cellular components (Figure 4A). As the major constituent of microtubules, tubulin beta protein is among the DEPs in brain which is involved in structural molecule activity (Table 2). In the brain decreased expression of tubulin beta chain in the rotenone-exposed group is a significant finding as rotenone is known to depolymerize microtubules and increase tubulin degradation (Ren et al.,2003). Neurofilament light chain b (Nef1b) is another DEP detected in the brain which as a cytoskeletal component of neurons provides structural support, and maintains the size and shape of the axons (Table 2) (Wang et al., 2018). In our study calretinin is another rotenone-induced DEP that significantly responded to erucic acid treatment (Table 2). Calretinin is present in both the central nervous system and the peripheral nervous system of zebrafish and was reported to protect dopaminergic neurons against degeneration in PD (Levanti et al., 2008; Mouatt-Prigent et al., 1994). In the intestines molecular functions and biological processes of rotenone-induced DEPs included mainly the catalytic enzyme activities, transport, and localization (Figure 4B).

The physical connection between cells and the ECM is maintained through multi-component molecular structures that are regulated by integrins. Talin is an adhesion protein that participates in the activation of integrins and connects them with the actin cytoskeleton (Zhao et al., 2022). We determined that erucic acid restored intestinal talin expression disrupted by rotenone which may help to maintain cytoskeletal integrity (Table 3).

STRING enrichment results showed that proteins involved in metabolic pathways were highly represented. Among these neuronal proteins, Nme4 and Ak1 and proteins involved in calcium and lipid transport activity were differentially expressed in brain tissues. Adenylate kinases (AKs) and nucleoside diphosphatase kinases (NMEs) add phosphate groups to nucleosides

leading to the formation of nucleotides. The AK family has seven members, associated with different tissues, including the brain, and AKs have a role in the phosphorylation of AMP to ADP an,d dAMP to dATP, as well as regulating a variety of intracellular and extracellular processes including nuclear transport, DNA synthesis and repair, and energy metabolism (Dzeja and Terzic, 2009). The NME family is involved in the conversion of nucleotide diphosphates to nucleotide triphosphates via phosphorylation. Differentially expressed Nme4 and Ak1 in the brain may be related to the alterations in purine metabolism due to rotenone exposure as Garcia-Esparcia et al., (2015) showed region-dependent changes in the expression of AK and NME family member genes involved in purine metabolism in PD.

We applied GO analysis to identify the biological processes and molecular functions of the differentially expressed proteins in response to erucic acid treatment and found that erucic acid treatment affected the expressions of proteins playing a role in phospholipase inhibitor activity, lipase inhibitor activity, carboxypeptidase activity, cAMP-dependent protein kinase regulator activity, and enzyme inhibitor activity, which are enriched in relation to protein phosphorylation, response to stimulus and lipid transport processes. Among the other affected proteins, sncga (gamma synuclein) is implicated in Lewy body dementia which is a characteristic of PD (Wang et al., 2017). Rhot2 has also been affected by erucic acid treatment. Rhot2 is involved in mitochondrial homeostasis and apoptosis in PD (Safiulina et al., 2019). ATP5 is a regulated protein detected at least in two different proteomic studies using the same sample type (Basso et al., 2004; Licker et al., 2012). In our study, the interaction network showed that atp6v1g1 and cox6a1 which functions in oxidative phosphorylation interacted with proteins involved in energy metabolism.

Oxidative phosphorylation and energy metabolism are determined as affected pathways as increased stress caused by ROS generation is one of the postulated causes for the death of dopaminergic neurons in PD. Mitochondria are the primary source of energy in the cell, producing ATP through respiration and oxidative phosphorylation, and also the principal generator of ROS, which may lead to intracellular oxidative stress (Subramaniam and Chesselet). The ETC's complex I and, to a lesser extent, complex III are thought to be the primary sources of ROS generation in mitochondria (Murphy, 2009; Subramaniam and Chesselet).

Immunohistochemical TH analysis was performed to evaluate the degeneration of dopaminergic neurons. Rotenone administration decreased TH+ cells, which reflected the loss of dopaminergic neurons observed in PD patients. The decrement in dopaminergic neurons in the rotenone group was increased by erucic acid administration. While degenerative alterations

in the midbrain are to blame for motor symptoms, extranigral pathology is linked to a variety of non-motor symptoms in PD. As a result, gastrointestinal (GI) dysfunction is a key nonmotor symptom of PD that can be seen at an early stage of the disease, even years before motor symptoms arise. We have previously reported lower locomotor activity, dopamine and serotonin levels, elevated DOPAC and DOPAC / dopamine levels in the brain, as well as disrupted oxidant-antioxidant equilibrium in the intestines and brain of rotenone-exposed zebrafish (Unal et al., 2019; Unal et al., 2020; Yurtsever et al., 2020; Cansız et al., 2021).

One of the major risk factors that may start or accelerate the degeneration of DA neurons is oxidative stress (Saravanan et al., 2006). As TH is the primary target of oxidative and nitrosative damage, to determine the relationship between degeneration in dopaminergic neurons and oxidative stress, we examined LPO and No as oxidative damage markers and Sod as the antioxidant enzyme. Validating our earlier findings, rotenone exposure led to increased LPO and No levels both in the brain and intestines. Increased No in the intestine shows that, NO as an enteric transmitter that leads to stress by inducing excessive nitrosylation and free radicals on neurons, is a component of oxidative stress induced by rotenone. Erucic acid was shown to attenuate inflammation in several physiological and pathological conditions through altering inflammatory mediators production and modulating neutrophils infiltration (Farag and Gad, 2022). Consistent with this role of NO, in our study erucic acid treatment in the rotenone group led to decreased intestinal and brain No levels.

In our present study, rotenone led to increased brain Sod activity. Sod upregulation in response to rotenone may be suggested to be an indicator of the brain's antioxidative defense system against oxidative stress. Accordingly, increased Sod activity may have prevented further increases in brain LPO. This finding has also been confirmed by an earlier report in rotenone-induced, oxidative stress-mediated dopaminergic neurodegeneration in rats (Saravanan et al., 2006). Erucic acid ameliorated the increased oxidative stress by lowering LPO and No levels both in the brain and intestines. Erucic acid treatment in the rotenone group led to a further increase in Sod activity in the brain. On the other hand, the major metabolic step in peroxisomes that contributes to the generation of H_2O_2 is fatty acid oxidation and, in the livers of rats fed high-erucic-acid rapeseed oil, peroxisomal-oxidation was shown to be dramatically increased (Schrader and Fahimi, 2006; Cehn et al., 2020). Accordingly, in our study, reduced intestinal Sod activity in erucic acid-treated fish is most likely owing to a compensatory reaction to prevent an increase in intestinal LPO.

GST enzyme activity, gene expressions, and genetic polymorphisms have all been studied in relation to PD since these enzymes are involved in the detoxification and metabolism of a

variety of environmental toxins and xenobiotics that may be linked to PD (Ozdamar, E.D., Can-Eke, 2013). Therefore, to examine the effect of erucic acid on the detoxification mechanism in dopaminergic neuron damage induced by rotenone, we investigated Gst activity in brain and intestinal tissues. Erucic acid improved Gst activity both in the brain and intestines. Rotenone exposure decreased Gst activity in the brain. On the other hand, in the erucic acid-treated rotenone group, Gst activity increased when compared to both the erucic acid group and the rotenone group, which may be attributed to the potentiation of the antioxidant response to rotenone toxicity in the presence of erucic acid as GST appears to be a promising enzymatic marker for detecting either endogenous or external oxidative stress (Vehovszky et al., 2010).

The antioxidant activity of erucic acid may be explained through the action of PGC-1α which is a PPARγ coactivator. PGC-1α has been shown to form heteromeric complexes with PPARδ to control mitochondrial proliferation and respiration and stimulate the expression of antioxidant enzymes including mitochondrial Mn-SOD, catalase, and glutathione peroxidase-1 (Chaturvedi and Beal, 2008).

Bone loss is a characteristic sign of PD, which is multifactorial and a result of motor dysfunction, causing immobility and decreased muscular strength. Accordingly, due to increased osteoclastogenesis and reduced bone formation, neurotoxin-induced dopaminergic degeneration resulted in bone loss (Handa et al., 2019). In our study Alp activity was evaluated as an early marker of osteoblast differentiation to examine the relationship between the deterioration in locomotor activity due to rotenone toxicity, which is characterized by reduced average speed and exploration rate, and osteoblast differentiation. Erucic acid treatment in the rotenone group ameliorated Alp levels which was more evident in the brain.

Increased AChE levels lower acetylcholine (ACh) levels to maintain the balanced cholinergic and dopaminergic systems, which is necessary for appropriate basal ganglia function (Zhou et al., 2003). In our study erucic acid treatment in the rotenone group normalized AChE activities in the intestines.

We have previously shown that rotenone impaired oxidant/antioxidant balance both in the brain and intestines in zebrafish (Unal et al., 2019). In our current study, to evaluate the effects of rotenone and erucic acid treatments on the expressions of genes associated with mitochondrial functions in PD, we determined the expressions of *lrrk2, park2, park7, and pink1* as the PD-related genes. The mutations in *lrrk*, *park7* and *pink1* are associated with familial PD. Lrrk2 mutations induce mitochondrial malfunction and Lrrk2 expression also activates the formation of ROS in cells (Subramaniam and Chesselet, 2013). Pink1 maintains mitochondrial morphology and protects neurons from ROS (Wang et al.,2011). In our study, erucic acid

treatment alone led to significant increases in the expressions of *lrrk2*, *park2, park7,* and *pink1.* This can be due to the antioxidant activity of erucic acid stimulating the expression of antioxidant enzymes through the action of PGC-1α (Chaturvedi and Beal, 2008) as Park 7 has a neuroprotective effect (Thomas et al., 2011). Diminished Park7 expression causes increased ROS, reduced mitochondrial membrane potential, and accumulated dysfunctional mitochondria, which can be ameliorated by increased Park2 (Li et al., 2021). Decreased LRRK2 in macrophages leads to oxidative stress and mitochondrial fragmentation (Weindel et al., 2020). On the other hand, the increased expressions of *lrrk2*, *park2, park7,* and *pink1* in the rotenone-treated group may be attributed to the defense mechanism against rotenone-induced oxidative stress. Increased *lrrk, park7,* and *pink1* expressions in the rotenone group were decreased by erucic acid treatment due to its protective effect against oxidative damage.

The effects of different PPARδ-ligand agonists such as L-165041 and GW501516 have been investigated and shown to be protective against cell damage and MPTP induced neurotoxicity (Iwashita et al., 2007). In another study, PPARδ-antagonist GSK0660 was found to protect cells against the effects of MPP^+ (Martin et al., 2013). PPARδ agonist, GW501516, has also been shown to be effective to improve locomotor activity, protect dopaminergic neurons from neurodegeneration and decrease ER stress in rotenone-induced PD in rats (Tong et al., 2016). Chen et al., 2019 showed that GW501516 significantly decreased MDA levels and increased SOD and catalase activities in PD induced mice (Chen et al., 2019).

Today, the molecular mechanisms responsible for the systemic molecular pathology of PD have gained enormous significance in the gut-brain axis in particular. In line with the results of the studies with PPARδ agonists, when we used erucic acid as a PPARδ-ligand in neurotoxin-induced PD model in zebrafish, we observed amelioration in TH expression and the expressions of PD-related genes in brain and rescued locomotor activity which can be attributed to improved oxidant-antioxidant status in both brain and intestines. Proteomic analysis results showed significantly dysregulated proteins both in the intestines and brain tissues of rotenone-exposed zebrafish and erucic acid treatment corrected the changes in the expression of proteins associated mainly with cytoskeletal organization, transport and localization. We believe that our study will shed light on the mechanism of the effects of PPARδ agonists and ω9-fatty acids in the gut-brain axis of PD.

On the other hand, the underlying mechanisms of some of the effects caused by erucic acid and their possible consequences should be examined in more detail. Erucic acid treatment led to lower intestinal No levels. The potential sources of NO in the gut include intrinsic intestinal tissue like the mast cells, epithelium, smooth muscle cells, and resident/infiltrating leukocytes.

Brain expresses nitric oxide synthase under resting conditions whereas, inflammatory stimuli are required for the induction of the inducible type (Salzman, 1995). Accordingly, the mechanism and consequences of decreased intestinal No levels due to erucic acid need to be examined in more detail in terms of intestinal hemostasis. Erucic acid increased brain Gst and Sod activity which may be due to the stimulation of protective defense systems. Similarly, by stimulating antioxidant mechanisms, erucic acid treatment alone increased *lrrk2*, *park2*, *park7*, and *pink1* expressions. Increased intestinal AChE activity is another issue that needs to be examined as AChE is effective in maintaining the balance between the cholinergic and dopaminergic systems. In our upcoming investigations, we intend to continue our research by carefully analyzing these routes.

Acknowledgement

This study was supported by Marmara University Scientific Research Projects Commission, Project no: TDK-2022-10377. We would like to thank the University of Health Sciences for supporting the proteomic analysis.

REFERENCES

An, H., Williams, N. G., Shelkovnikova, T. A. (2018). NEAT1 and paraspeckles in neurodegenerative diseases: A missing lnc found?. Non-coding RNA research, 3(4), 243–252.

Altinoz, M.A., Ozpinar, A., (2019) PPAR-delta and erucic acid in multiple sclerosis and Alzheimer's Disease. Likely benefits in terms of immunity and metabolism. Int. Immunopharmacol., 69, 245–256.

Altinoz, M.A., Elmaci, İ., Hacimuftuoglu, A., Ozpinar, A., Hacker, E., Ozpinar, A., (2021). PPARδ and its ligand erucic acid may act anti-tumoral, neuroprotective, and myelin protective in neuroblastoma, glioblastoma, and Parkinson's disease. Mol Aspects Med.,78,100871.

Bankhead, P., Loughrey, M.B., Fernández, J.A., Dombrowski, Y., McArt, D.G., Dunne, P.D., et al.,(2017) QuPath: Open source software for digital pathology image analysis. Sci Rep,7. doi:10.1038/S41598-017-17204-5.

Bartel, W.P., Van Laar, V.S., Burton, E.A., (2020) Parkinson's disease. Behav Neural Genet Zebrafish, 377–412.

Basso, M., Giraudo, S., Corpillo, D. et al. (2004) Proteome analysis of human substantia nigra in Parkinson's disease. Proteomics, 4 (12):3943–3952.

Cansız, D., Ünal, İ., Üstündağ, Ü.V., Alturfan, A.A., Altinoz, M.A., Elmacı, İ., Emekli-Alturfan, E., (2021) Caprylic acid ameliorates rotenone induced inflammation and oxidative stress in the gut-brain axis in Zebrafish. Mol Biol Rep.,48(6):5259-5273

Chaturvedi, R.K., Beal, M.F., (2008). PPAR: a therapeutic target in Parkinson's disease. J. Neurochem. 106 (2), 506–518.

Chen, L., Xue, L., Zheng, J., Tian, X., Zhang, Y., Tong, Q., (2019). PPARß/δ agonist alleviates NLRP3 inflammasome-mediated neuroinflammation in the MPTP mouse model of Parkinson's disease. Behav. Brain Res. 356, 483–489.

Chen, X., Shang, L., Deng, S., Li, P., Chen, K., Gao, T., Zhang, X., Chen, Z., Zeng, J., (2020) Peroxisomal oxidation of erucic acid suppresses mitochondrial fatty acid oxidation by stimulating malonyl-CoA formation in the rat liver. J Biol Chem. 24;295(30):10168-10179.

Dogra, N., Mani, R.J., Katare, D.P., (2022). The Gut-Brain Axis: Two Ways Signaling in Parkinson's Disease. Cell Mol Neurobiol.,42(2):315-332.

Dzeja, P., Terzic, A., (2009) Adenylate kinase and AMP signaling networks: metabolic monitoring, signal communica- tion and body energy sensing. Int J Mol Sci., 10: 1729–72

EFSA., (2016). Scientific opinion on erucic acid in feed and food. EFSA J. , 14, 1–173.

Ellman, (1961) A new and rapid colorimetric determination of acetylcholinesterase activity. Biochem Pharmacol., (61),90145-9.

Farag, M.A., Gad, M.Z., (2022) Omega-9 fatty acids: potential roles in inflammation and cancer management. J Genet Eng Biotechnol. 16;20(1):48.

Fox A.H. (2018) Paraspeckles: where long noncoding RNA meets phase separation. Trends Biochem. Sci. 43(2):124–135

Garcia-Esparcia, P., Hernández-Ortega, K., Ansoleaga, B., Carmona, M., Ferrer, I. (2015) Purine metabolism gene deregulation in Parkinson's disease. Neuropathol Appl Neurobiol. ,41(7):926-40.

Haavik, J., Toska, K. (1998) Tyrosine hydroxylase and Parkinson's disease. Mol Neurobiol.16(3):285-309.

Habig, W.H., Jacoby, W.B. (1981) Assays for differentation of glutathion-s- transferases. Methods Enzymol, 77:398–405

Handa, K., Kiyohara, S., Yamakawa, T., Ishikawa, K., Hosonuma, M., Sakai, N., Karakawa, A., Chatani, M., Tsuji, M., Inagaki K, Kiuchi Y, Takami M, Negishi-Koga T., 2019. Bone loss caused by dopaminergic degeneration and levodopa treatment in Parkinson's disease model mice. Sci Rep, 24;9(1):13768.

Heberle, H., Meirelles, G.V., da Silva, F.R., Telles, G.P., Minghim, R., (2015) InteractiVenn: a web-based tool for the analysis of sets through Venn diagrams. BMC Bioinformatics. 22;16(1):169.

Hein, A.L., Mukherjee, M., Talmon, G.A., Natarajan, S.K., Nordgren, T.M., Lyden, E., et al., (2021) QuPath Digital Immunohistochemical Analysis of Placental Tissue. J Pathol Inform. ;12:40.

Hogan, A.L., Grima, N., Fifita, J.A., McCann, E.P., Heng, B., Fat, S.C.M., Wu, S., Maharjan, R., Cain, A.K., Henden, L., Rayner, S., Tarr, I., Zhang, K.Y., Zhao, Q., Zhang, Z.H., Wright,

A., Lee ,A., Morsch, M., Yang, S., Williams, K.L., Blair, I.P., (2021) Splicing factor proline and glutamine rich intron retention, reduced expression and aggregate formation are pathological features of amyotrophic lateral sclerosis. Neuropathol Appl Neurobiol.,47(7):990-1003.

Iwashita, A., Muramatsu, Y., Yamazaki, T., Muramoto, M., Kita, Y., Yamazaki, S., Mihara, K., Moriguchi, A., Matsuoka, N., (2007). Neuroprotective efficacy of the peroxisome proliferator-activated receptor delta-selective agonists in vitro and in vivo. J. Pharmacol. Exp. Therapeut. 320 (3), 1087–1096.

Kahremany, S., Livne, A., Gruzman, A., Senderowitz, H., Sasson, S., (2015) Activation of PPARδ: from computer modelling to biological effects. Br J Pharmacol. 172(3):754-70.

Kasap, M., Akpinar, G., Kanli, A., (2017) Proteomic studies associated with Parkinson's disease. Expert Rev Proteomics, 14(3):193-209.

Kaslin, J., Panula, P., (2001) Comparative anatomy of the histaminergic and other aminergic systems in zebrafish (Danio rerio). J Comp Neuroli, 440:342–77.

Levanti, M.B., Montalbano, G., Laurà, R., Ciriaco, E., Cobo, T., García-Suarez, O., Germanà, A., Vega, J.A., (2008). Calretinin in the peripheral nervous system of the adult zebrafish. J Anat. 212(1):67-71.

Li W, Fu Y, Halliday GM, Sue CM (2021). PARK Genes Link Mitochondrial Dysfunction and Alpha-Synuclein Pathology in Sporadic Parkinson's Disease. Front Cell Dev Biol. 6;9:612476.

Licker, V., C., te M., Lobrinus, J.A., et al. (2012) Proteomic profiling of the substantia nigra demonstrates CNDP2 overexpression in Parkinson’s disease. J Proteomics.75(15):11.

Livak, K.J., Schmittgen, T.D. (2001) Analysis of relative gene expression data using real-time quantitative PCR and the 2−ΔΔCT method. Methods, 25,402–408.

Lowry, O.H., Rosebrough, N.J., Farr, A.L., Randall, R.J. (1951) Protein measurement with the Folin phenol reagent. J Biol Chem, 193:265–275

Maere, S., Heymans, K., Kuiper, M., (2005) BiNGO: a Cytoscape plugin to assess overrepresentation of gene ontology categories in biological networks. Bioinformatics. 15;21(16):3448-9.

Martin, H.L., Mounsey, R.B., Sathe, K., Mustafa, S., Nelson, M.C., Evans, R.M., Teismann, P., (2013). A peroxisome proliferator-activated receptor-δ agonist provides neuroprotection in the 1-methyl-4-phenyl-1,2,3,6-tetrahydropyridine model of Parkinson's disease. Neuroscience 240, 191–203.

Miranda, K.M., Espey, M.G., Wink, D.A. (2001) A rapid, simple spectrophotometric method for simultaneous detection of nitrate and nitrite. Nitric Oxide, 5:62–71

Mouatt-Prigent, A., Agid, Y., Hirsch, E.C., (1994). Does the calcium binding protein calretinin protect dopaminergic neurons against degeneration in Parkinson's disease? Brain Res. 30;668(1-2):62-70.

Murphy, M.P. (2009) How mitochondria produce reactive oxygen species. The Biochemical Journal, 417:1–13.

Mylorie, A.A., Collins, H., Umbles, C.,Kyle, J. (1986) Erythrocyte superoxide dismutase activity and other parameters of cupper status in rats ingesting lead acetate. Toxicol Appl Pharmacol,82:512–520.

Mysona, B.A., Segar, S., Hernandez, C., Kim, C., Zhao, J., Mysona, D., et al., (2020) QuPath Automated Analysis of Optic Nerve Degeneration in Brown Norway Rats. Transl Vis Sci Technol, 9.

Nadig, A., Jois, S.N., Prasad, K.N., Vinu, V. (2020) Locomotor Activities of Adult Zebrafish (Danio rerio) Under the Influence of Pranic Energy: Controlled Study. International Journal of Lakes and Rivers. 13 (1); 43-55.

Narendra D, Tanaka A, Suen DF, Youle RJ. Parkin is recruited selectively to impaired mitochondria and promotes their autophagy. J Cell Biol. 2008;183:795–803

Nury, T., Lizard, G., Vejux, A., (2020) Lipids Nutrients in Parkinson and Alzheimer's Diseases: Cell Death and Cytoprotection. Int J Mol Sci., 3;21(7):2501.

Nuytemans K, Theuns J, Cruts M, Van Broeckhoven C. Genetic etiology of Parkinson disease associated with mutations in the SNCA, PARK2, PINK1, PARK7, and LRRK2 genes: a mutation update. Hum Mutat. 2010 Jul;31(7):763-80. doi: 10.1002/humu.21277. PMID: 20506312; PMCID: PMC3056147

Ozdamar, E.D., Can-Eke, B., (2013) Glutathion-S-Transferases (GSTs) and Parkinson's disease in a MPTP-induced C57BL/6 mouse model. Mol Neurodegeneration, 8, P30.

Ren, Y., Zhao, J., Feng, J., (2003) Parkin binds to alpha/beta tubulin and increases their ubiquitination and degradation. J Neurosci., 15;23(8):3316-24.

Rodriguez, A., Zhang, H., Klaminder, J., Brodin, T., Andersson, P., & Andersson, M. 2018. ToxTrac: a fast and robust software for tracking organisms, Methods in Ecology and Evolution, 9(2018), 460-464.

Safiulina, D., Kuum, M., Choubey, V., Hickey, M.A., Kaasik, A., (2019) Mitochondrial transport proteins RHOT1 and RHOT2 serve as docking sites for PRKN-mediated mitophagy. Autophagy, 15(5):930-931.

Salzman, A.L. (1995) Nitric oxide in the gut. New Horiz. 3(1):33-45.

Saravanan, K.S., Sindhu, K.M., Senthilkumar, K.S., Mohanakumar, K.P., L-deprenyl protects against rotenone-induced, oxidative stress-mediated dopaminergic neurodegeneration in rats. Neurochem Int. 2006 Jul;49(1):28-40.

Schnegg, C.I., Robbins, M.E., (2011) Neuroprotective Mechanisms of PPARδ: Modulation of Oxidative Stress and Inflammatory Processes. PPAR Res.,:373560.

Schrader, M., Fahimi, H.D., 2006. Peroxisomes and oxidative stress. Biochim Biophys Acta. 1763(12):1755-66.

Sissener, N.H., Ørnsrud, R., Sanden, M., Frøyland, L., Remø, S., Lundebye, A.K., 2018. Erucic Acid (22:1n-9) in Fish Feed, Farmed, and Wild Fish and Seafood Products. Nutrients. 5;10(10):1443.

Subramaniam, S.R., Chesselet, M.F. (2013) Mitochondrial dysfunction and oxidative stress in Parkinson's disease. Prog Neurobiol, 106-107,17-32.

Sürmen, M.G., Sürmen, S., Cansız, D., Ünal, İ., Üstündağ, Ü.V., Alturfan, A.A., Emekli-Alturfan, E., (2021) Quantitative phosphoproteomics to resolve the cellular responses to octanoic acid in rotenone exposed zebrafish. J Food Biochem. 45(10):e13923.

Thomas, K. J., Mccoy, M. K., Blackinton, J., Beilina, A., Van Der Brug, M., Sandebring, A., et al. (2011). DJ-1 acts in parallel to the PINK1/parkin pathway to control mitochondrial function and autophagy. Hum. Mol. Genet. 20, 40–50.

Thomassen, M.S., Røsjø, C., (1989). Different fats in feed for salmon: Influence on sensory parameters, growth rate and fatty acids in muscle and heart. Aquaculture.,79:129–135.

Tong, Q., Wu, L., Gao, Q., Ou, Z., Zhu, D., Zhang, Y., (2016). Pparβ/δ agonist provides neuroprotection by suppression of ire1α-caspase-12-mediated endoplasmic reticulum stress pathway in the rotenone rat model of Parkinson's disease. Mol. Neurobiol. 53 (6), 3822–3831

Tyagi, S., Gupta, P., Saini, A.S., Kaushal, C., Sharma, S., (2011) The peroxisome proliferator-activated receptor: A family of nuclear receptors role in various diseases. J Adv Pharm Technol Res., 2(4):236-40.

UniProt Consortium., (2019) UniProt: a worldwide hub of protein knowledge. Nucleic Acids Res., 8;47(D1):D506-D515.

Ünal, İ., Çalışkan-Ak, E., Üstündağ, Ü.V.,Ateş, P.S., Alturfan, A.A., Altinoz, M.A., Elmaci, I., Emekli-Alturfan, E., (2020) Neuroprotective effects of mitoquinone and oleandrin on Parkinson's disease model in zebrafish. Int J Neurosci 130(6):574–582 23.

Ünal, İ., Üstündağ, Ü.V., Ateş, P.S., Eğilmezer, G., Alturfan, A.A., Yiğitbaşı, T., Emekli-Alturfan, E., (2019) Rotenone impairs oxidant/antioxidant balance both in brain and intestines in zebrafish. Int J Neurosci, 129(4):363–368.

Valente EM, bou-Sleiman PM, Caputo V, Muqit MM, Harvey K, Gispert S, Ali Z, Del TD, Bentivoglio AR, Healy DG, Albanese A, Nussbaum R, Gonzalez-Maldonado R, Deller T, Salvi S, Cortelli P, Gilks WP, Latchman DS, Harvey RJ, Dallapiccola B, Auburger G, Wood NW. Hereditary early-onset Parkinson's disease caused by mutations in PINK1. Science. 2004a;304:1158–1160.

Vehovszky, A., Szabó, H., Acs, A., Gyori, J., Farkas, A. (2010) Effects of rotenone and other mitochondrial complex I inhibitors on the brine shrimp Artemia. Acta Biol Hung. 61(4):401-10.

Wang, H.L., Chou, A.H., Wu, A.S., Chen, S.Y., Weng, Y.H., Kao, Y.C., Yeh, T.H., Chu, P.J., Lu, C.S. (2011) PARK6 PINK1 mutants are defective in maintaining mitochondrial membrane potential and inhibiting ROS formation of substantia nigra dopaminergic neurons. Biochimica et biophysica acta. 1812:674–684.

Walter, K., Schült, C., (1974) Acid and alkaline phosphatase in serum (two point method) In Methods of enzymatic Analysis Ed: Bergmeyer HU, 2nd ed. FL, p.856-886.

Wang Y. (2018) Genome-wide screening of NEAT1 regulators reveals cross-regulation between paraspeckles and mitochondria. Nat. Cell Biol. 20(10):1145–1158

Wang, S., Ji, D., Yang, Q., Li, M., Ma, Z., Zhang, S., Li, H. (2018) NEFLb impairs early nervous system development via regulation of neuron apoptosis in zebrafish. Journal of Cellular Physiology, 234(7):11208-11218

Wang, Y., Liu, W., Yang, J., Wang, F., Yizhen, S., Zhong, Z.M., Wang, H., Hu, L.F., Liu, C.F. (2017) Parkinson's disease-like motor and non-motor symptoms in rotenone-treated zebrafish. Neurotoxicology, 58:103-109.

Wauters, F., Cornelissen, T., Imberechts, D., Martin, S., Koentjoro, B., Sue, C., et al. (2020). LRRK2 mutations impair depolarization-induced mitophagy through inhibition of mitochondrial accumulation of RAB10. Autophagy 16, 203–222.

Weihofen A, Thomas KJ, Ostaszewski BL, Cookson MR, Selkoe DJ. Pink1 forms a multiprotein complex with Miro and Milton, linking Pink1 function to mitochondrial trafficking. Biochemistry. 2009;48:2045–2052.

Weindel, C. G., Bell, S. L., Vail, K. J., West, K. O., Patrick, K. L., and Watson, R. O. (2020). LRRK2 maintains mitochondrial homeostasis and regulates innate immune responses to Mycobacterium tuberculosis. Elife 9:e51071.

Wiśniewski, J.R., Zougman, A., Nagaraj, N., Mann, M., (2009) Universal sample preparation method for proteome analysis. Nat Methods, 6(5):359-62.

Xiong H, Wang D, Chen L, Choo YS, Ma H, Tang C, Xia K, Jiang W, Ronai Z, Zhuang X, Zhang Z. Parkin, PINK1, and DJ-1 form a ubiquitin E3 ligase complex promoting unfolded protein degradation. J Clin Invest. 2009;119:650–660.

Yagi K (1984) Assay for blood plasma or serum. Method enzymol 105:328–331.

Yurtsever, İ., Üstündağ, Ü.V., Ünal, İ., Ateş, P.S., Emekli-Alturfan, E. (2020) Rifampicin decreases neuroinflammation to maintain mitochondrial function and calcium homeostasis in rotenone-treated zebrafish. Drug Chem Toxicol, 13:1–8.

Zhang, L., Shimoji, M., Thomas, B., Moore, D.J., Yu, S.W., Marupudi, N.I., Torp, R., Torgner, I.A., Ottersen, O.P., Dawson, T.M., Dawson, V.L.(2005) Mitochondrial localization of the Parkinson's disease related protein DJ-1: implications for pathogenesis. Human molecular genetics. 14,2063–2073.

Zhao, Y., Lykov, N., Tzeng, C., (2022) Talin-1 interaction network in cellular mechanotransduction (Review). Int J Mol Med. 49(5):60.

Zhou, F. M., Wilson, C., and Dani, J. A. (2003) Muscarinic and nicotinic cholinergic mechanisms in the mesostriatal dopamine systems. Neuroscientist 9, 23– 36

AUTHOR CONTRIBUTIONS

Derya Cansız: Investigation, Methodology; **İsmail Unal**: Investigation, Methodology; **Merih Beler; Zehra Sezer; Mustafa Gani Sürmen, Saime Sürmen, Merih Beler, Ünsal Veli Üstündağ, Elif Güzel**: Methodology; **A. Ata Alturfan**: Writing-review & Editing; **Ebru Emekli-Alturfan**: Supervision; Data analysis; Writing-review & Editing.

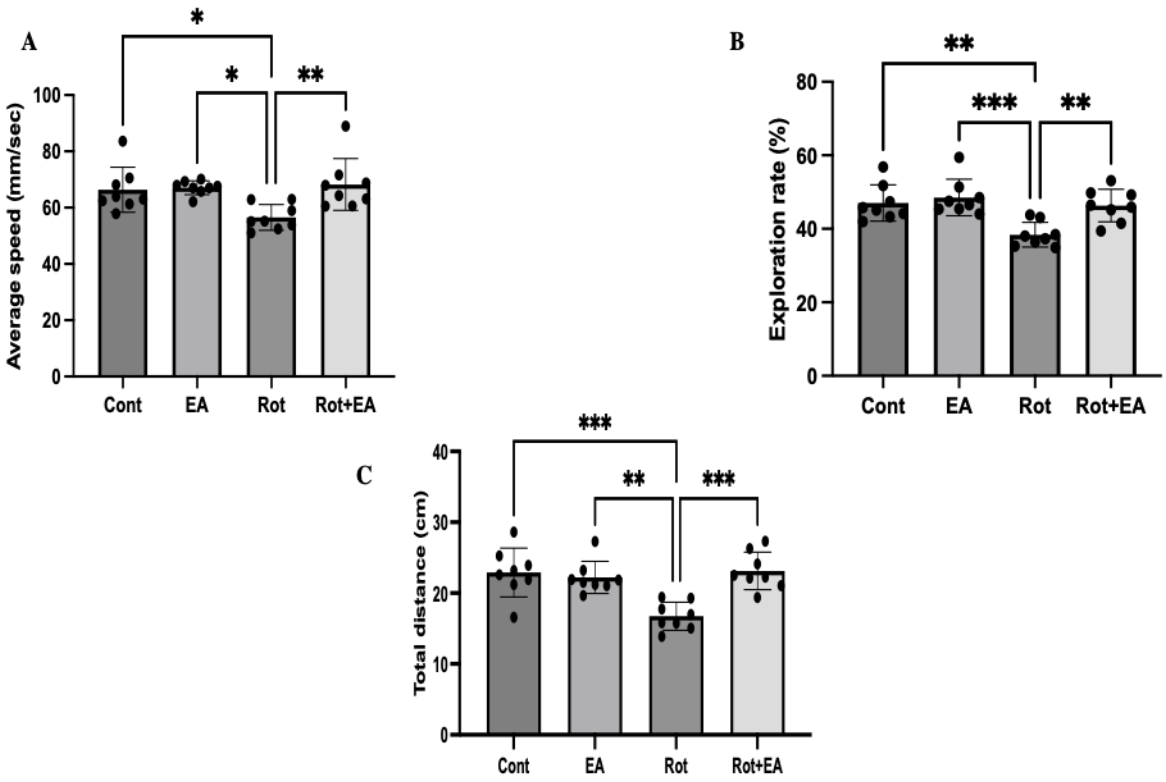

Figure 1: Locomotor activities of the groups are given as average speed (A) Exploration rate (B) and Total distance travelled (C) (n=8). Data presented are mean ± SD. Significant difference is indicated by an asterisk. *** $p<0.001$, ** $p<0.01$, ** $p<0.05$. Cont: Control Group; EA: Erucic Acid Group; Rot:Rotenone Group; Rot+EA: Rotenone+Erucic Acid Group

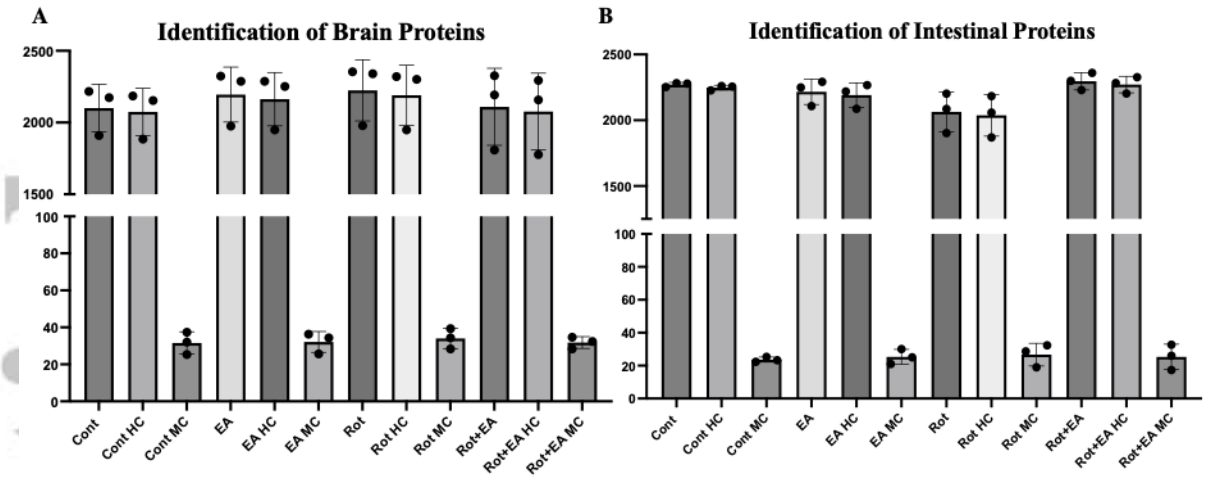

Figure 2: Protein identifications for each group. (A) Brain and (B) Intestine. Cont: Control Group; EA: Erucic Acid Group; Rot:Rotenone Group; Rot+EA: Rotenone+Erucic Acid Group; HC: High Confidence; MC: Medium Confidence

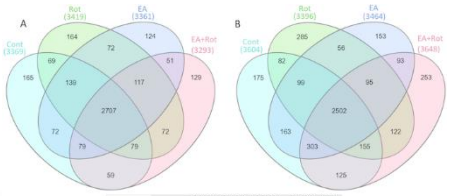

C

		The number of proteins shared with the controls	Not found in the controls
Brain	Rot	2994	425
	EA	2997	364
	EA+Rot	2924	369
Intestines	Rot	2838	558
	EA	3067	397
	EA+Rot	3085	563

Figure 3: The number of proteins for each treatment groups. (A) Brain (B) Intestine (C) Common proteins. Proteins identified with high confidence, < 1% FDR.

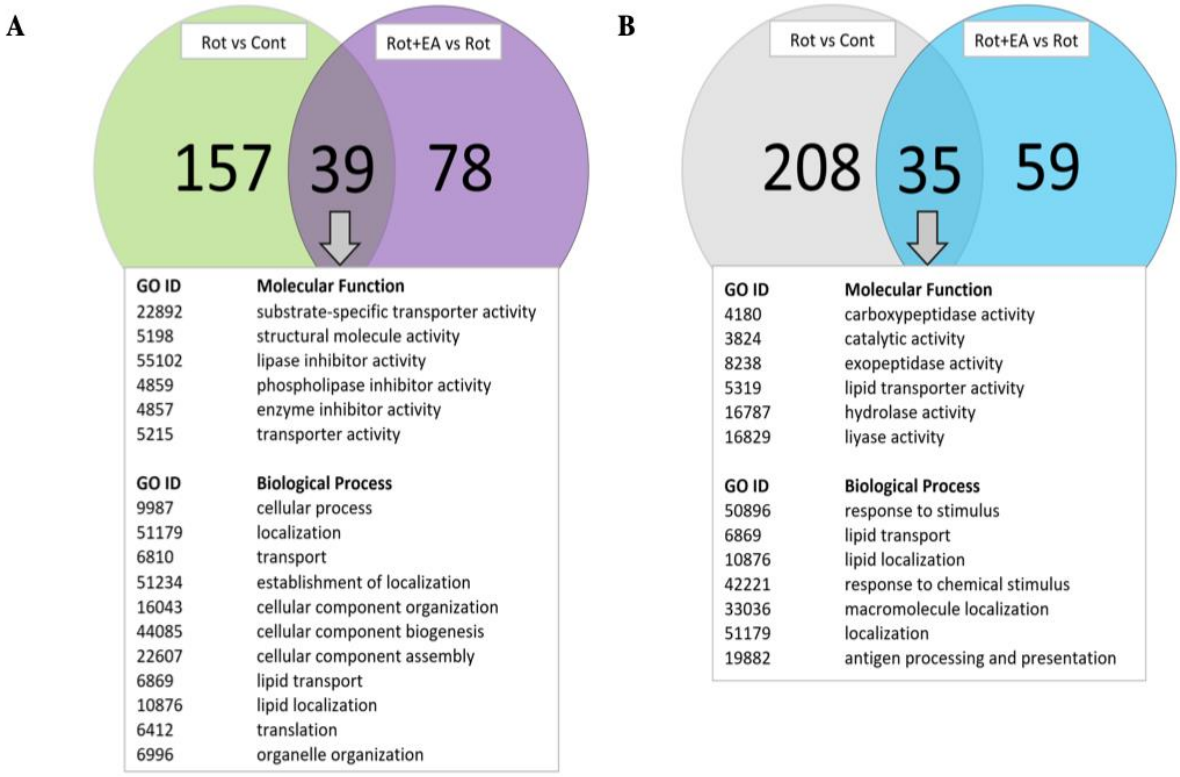

Figure 4. Common differentially expressed proteins (DEPs) in the groups, (A) Brain and (B) Intestine. The bottom panel indicates the common molecular programs affected by rotetone and erucic acid treatment.

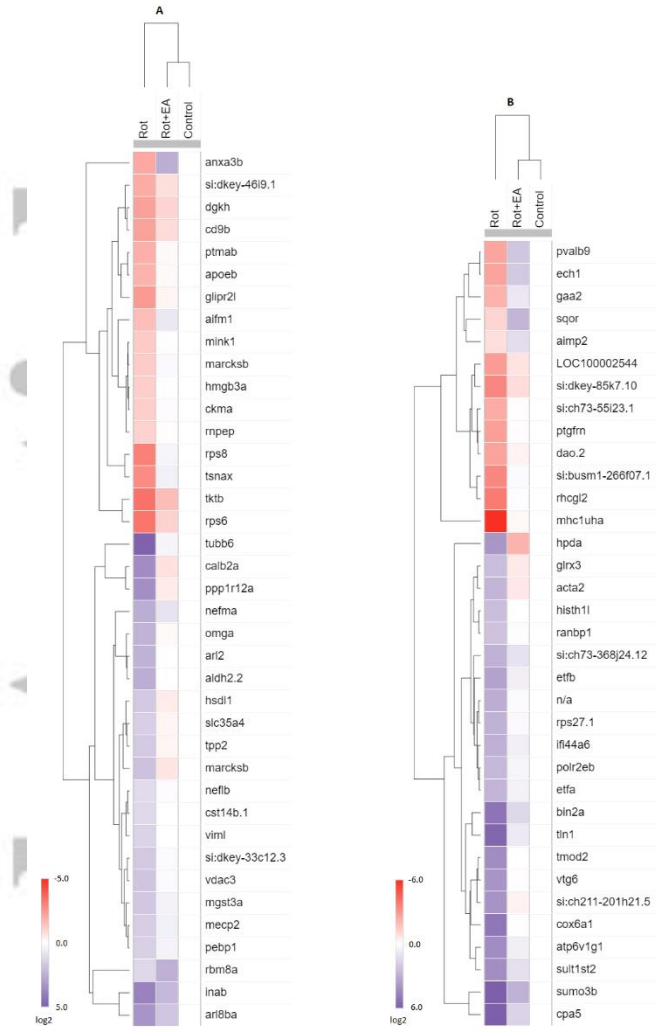

Figure 5. Heatmap showing the abundances of erucic acid treatment-responsive proteins in the control, rotenone and erucic acid groups in (A) Brain and (B) Intestine. The heatmap was constructed using the Morpheus program (Morpheus, https://software.broadinstitute.org/morpheus). The heatmap was scaled according to the z-score before clustering. More than 2-fold with statistical significance, at least two peptides. N/A: represents the protein with the accession number A0A0G2L2U8.

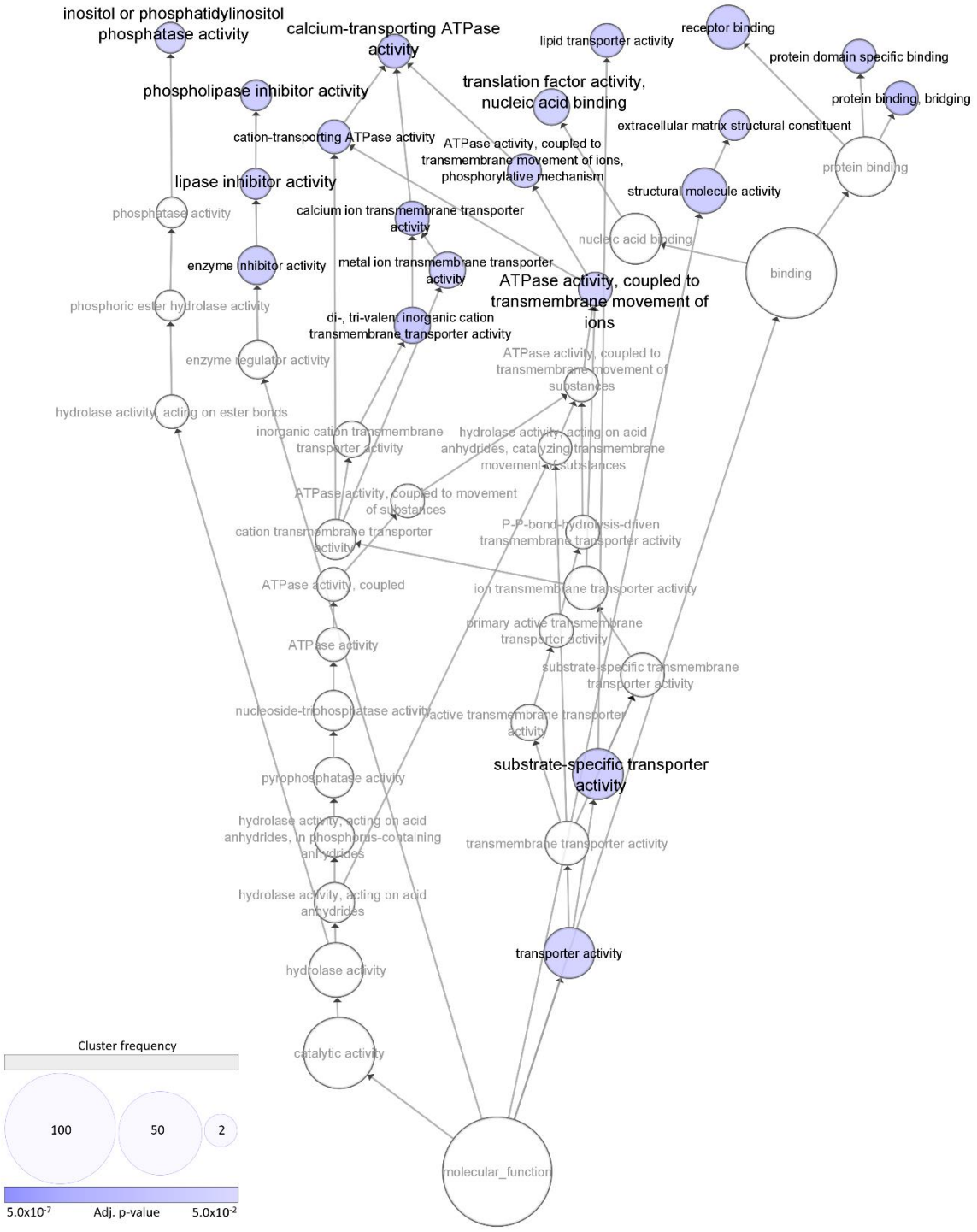

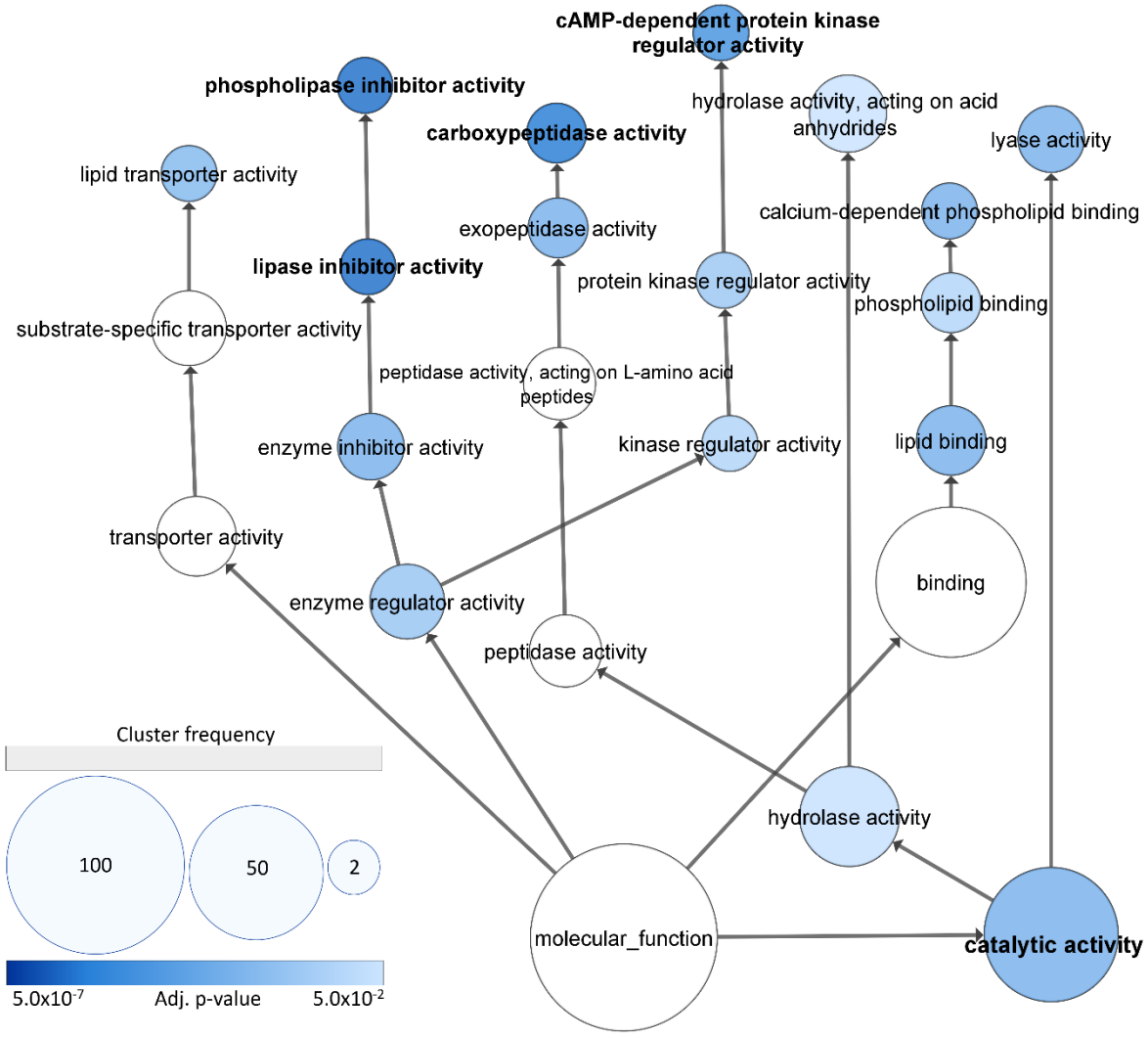

Figure 6. GO enrichment analysis of (A) Brain and (B) Intestine. Molecular function of dysregulated proteins (196 proteins for brain and 243 proteins for intestinal tissues) analyzed by using the Cytoscape program for annotation and visualization. Size and color depth of the circles indicate the cluster frequency and adj. p-value

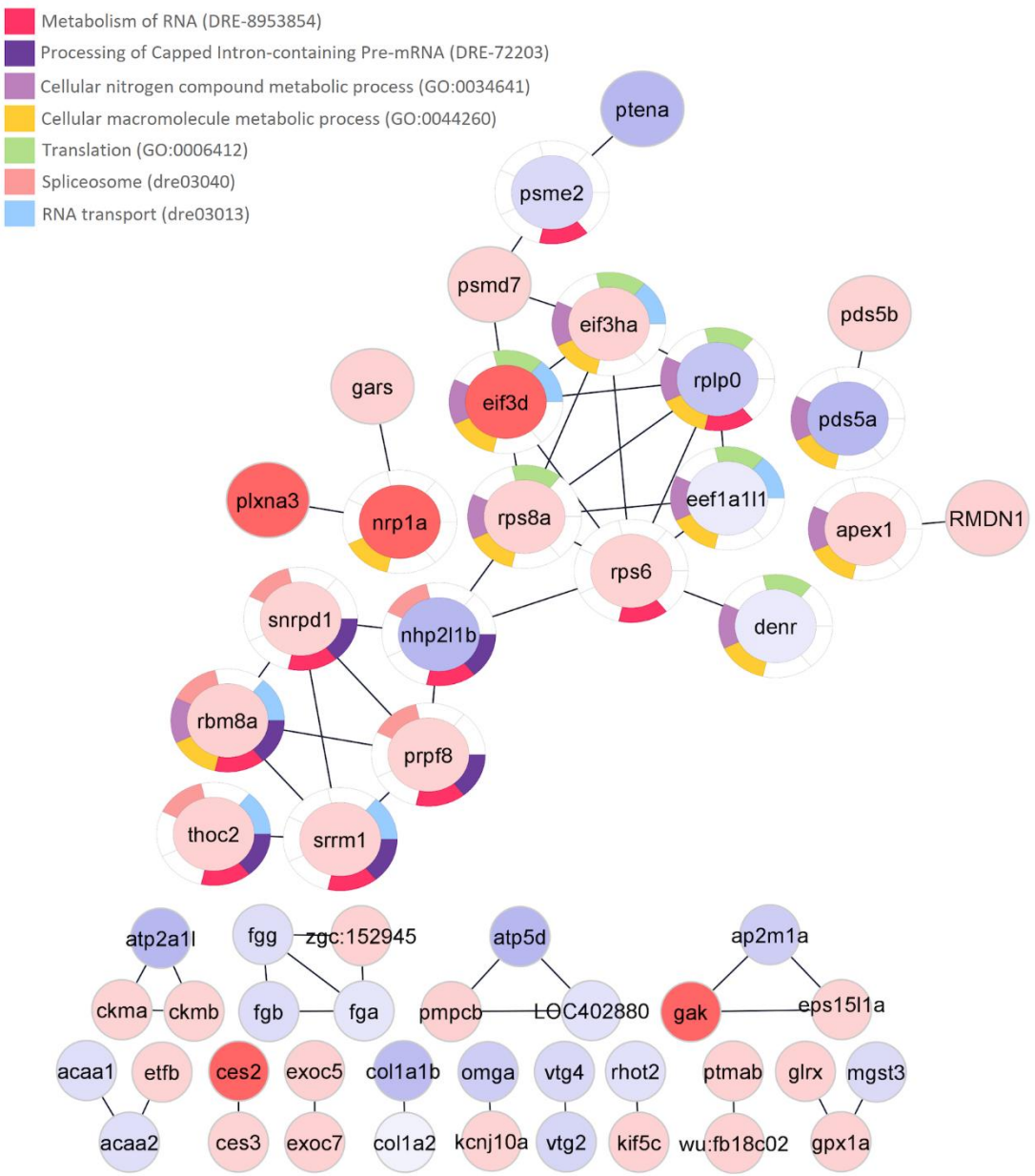

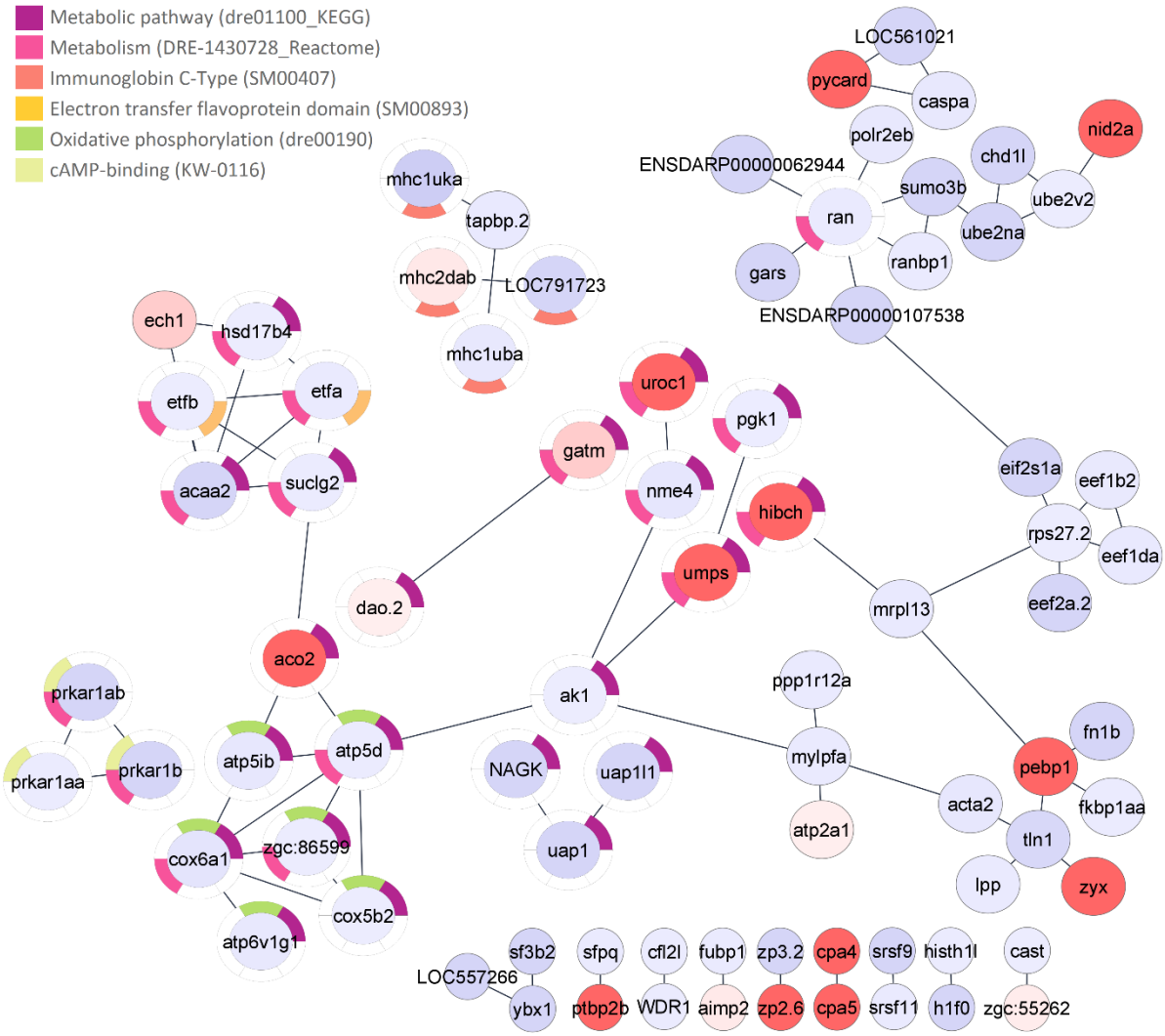

Figure 7. **Protein-protein interactions of (**A) Brain (B) Intestine**.** The network formed with differentially expressed proteins in rotenone compared to control. Amino acid sequences of 243 protein (for intestine) and 196 proteins (for brain) were uploaded to STRING database and applied a high-confidence filter with interaction score 0.07. Network stats for intestine and brain; average node degree: 0.681, 0.644; avg. local clustering coefficient: 0.256, 0.261 and PPI enrichment p-value: 1.94e-^{06}, 0.0102, respectively. Color depth of the nodes represent expression differences. Downregulated proteins were indicated by lilac color, and upregulated proteins were indicated by red color. Colored node borders indicate protein features based on functional enrichment analysis.

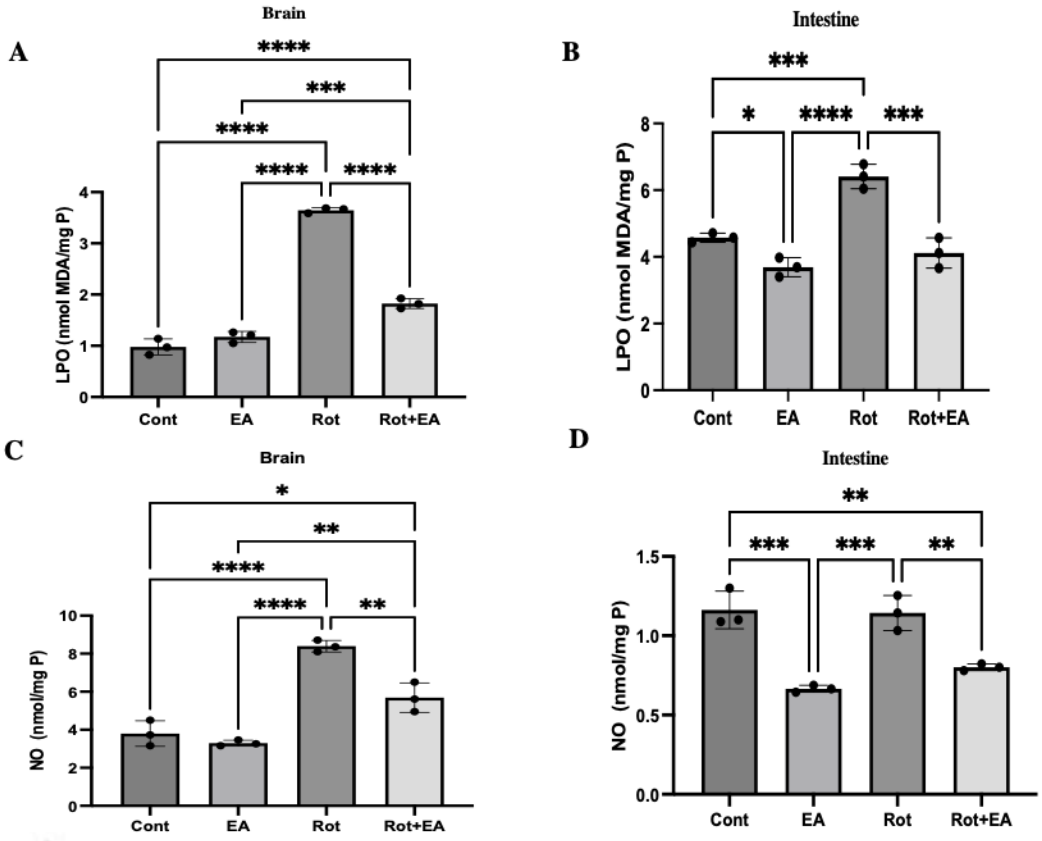

Figure 8: Brain and intestinal lipid peroxidation (LPO) levels (A,B) (nmol MDA/mg P) and nitric oxide (NO) levels (C,D) (nmol/mg P) of the groups. Data presented are mean ± SD. Significant difference is indicated by an asterisk. **** p<0.0001, *** p<0.001, ** p<0.01, * p<0.05. Cont: Control Group; EA: Erucic Acid Group; Rot:Rotenone Group; Rot+EA: Rotenone+Erucic Acid Group

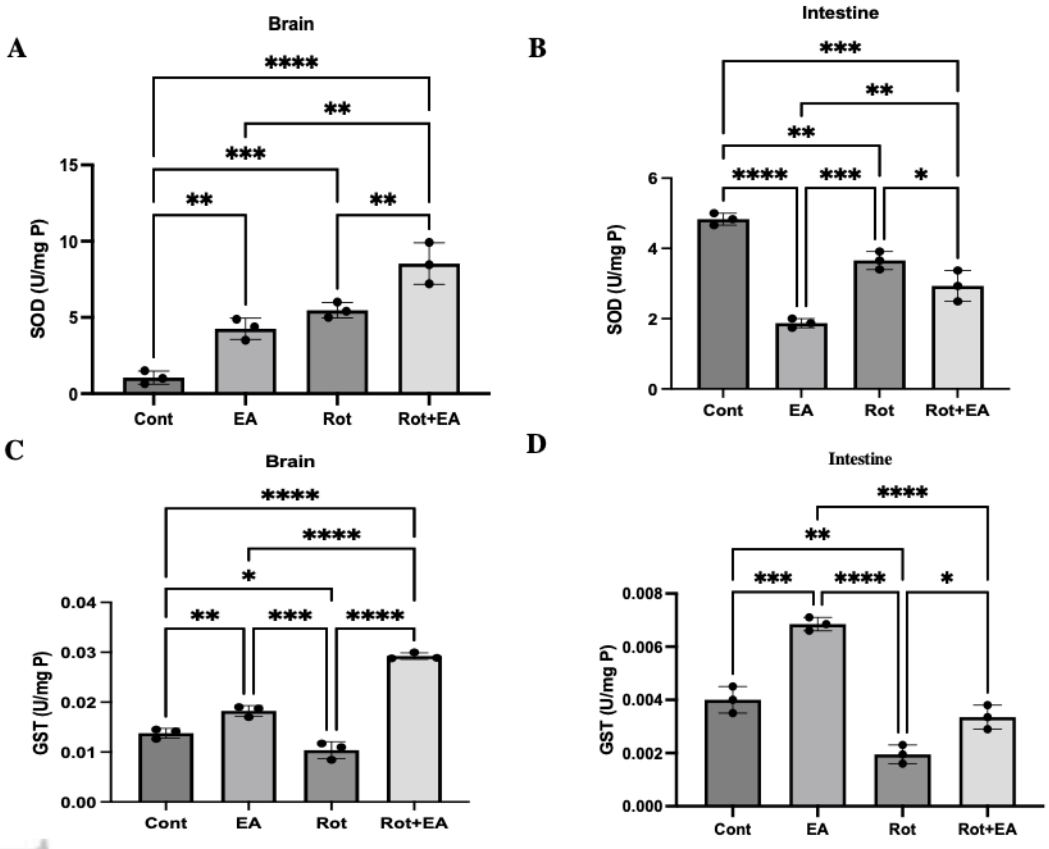

Figure 9: Brain and intestinal superoxide dismutase (Sod) activities (A,B) (U/ mg P) and glutathione-S- transferase (GST) activities (C,D) (U/ mg P) of the groups. Data presented are mean ± SD. Significant difference is indicated by an asterisk. **** p<0.0001, *** p<0.001, ** p<0.01, * p<0.05 Cont: Control Group; EA: Erucic Acid Group; Rot:Rotenone Group; Rot+EA: Rotenone+Erucic Acid Group

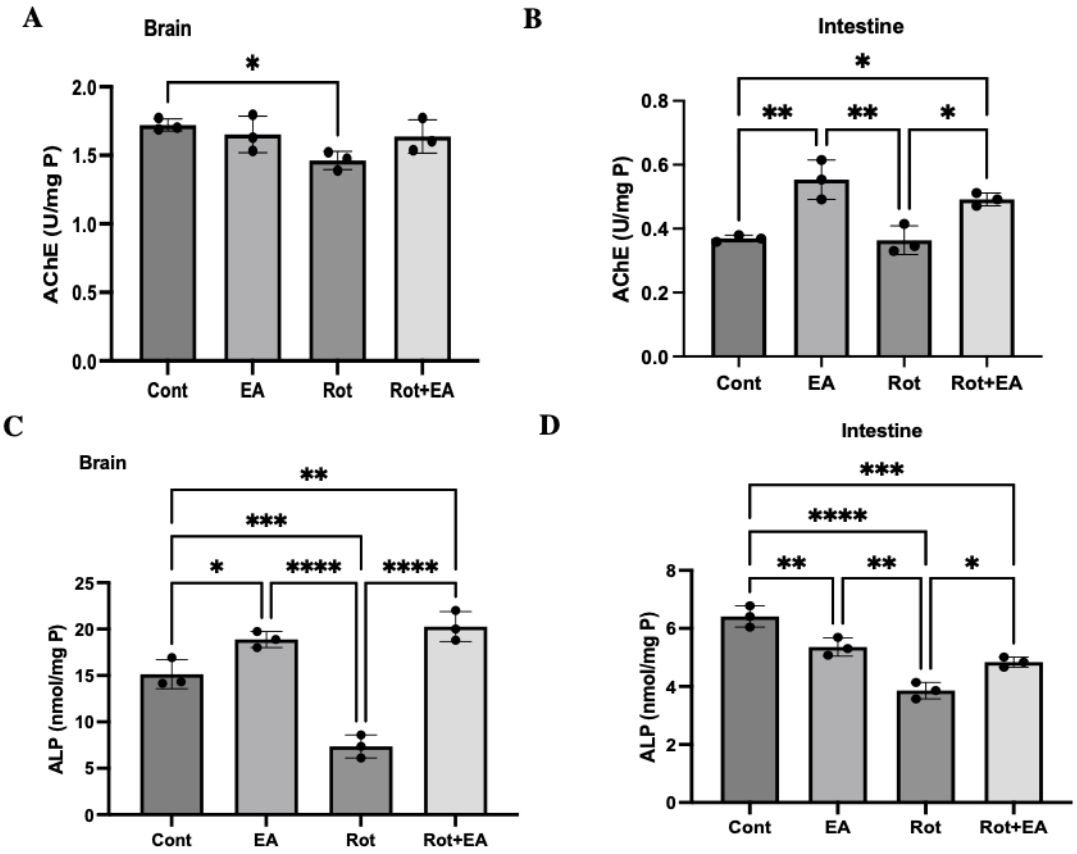

Figure 10: Brain and intestinal acetylcholinesterase (AChE) activities (U/ mg P) (A,B) and alkaline phosphatase (Alp) levels (nmol/mg P) (C,D) of the groups. Data presented are mean ± SD. Significant difference is indicated by an asterisk. **** $p<0.0001$, *** $p<0.001$, ** $p<0.01$, * $p<0.05$. Cont: Control Group; EA: Erucic Acid Group; Rot:Rotenone Group; Rot+EA: Rotenone+Erucic Acid Group

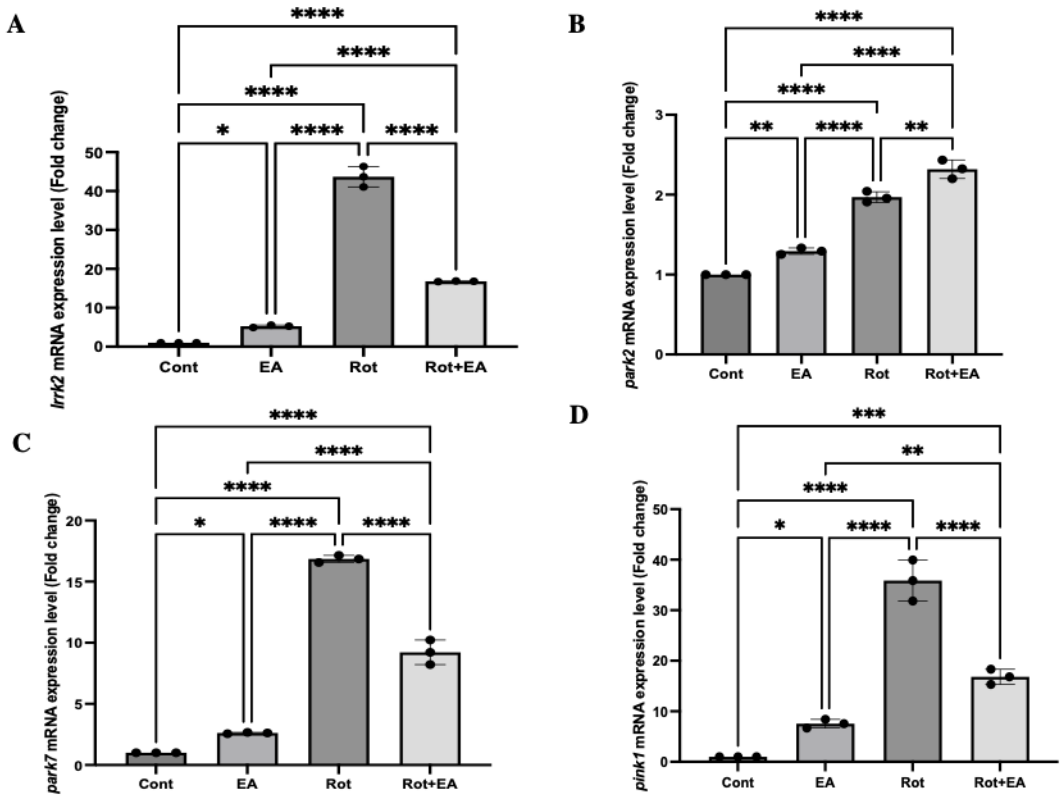

Figure 11: Bar graph presentation of the fold change of brain *lrrk2* (A), *park2* (B), *park7* (C) and *pink1* (D) transcripts quantified by RT-PCR. All RT-PCR results are normalized to β-actin, the house keeping gene and expressed as change from their respective controls. The average values were obtained from three experiments. Data presented are mean ± SD. **** $p<0.0001$, *** $p<0.001$, ** $p<0.01$, * $p<0.05$. Cont: Control Group; EA: Erucic Acid Group; Rot:Rotenone Group; Rot+EA: Rotenone+Erucic Acid Group

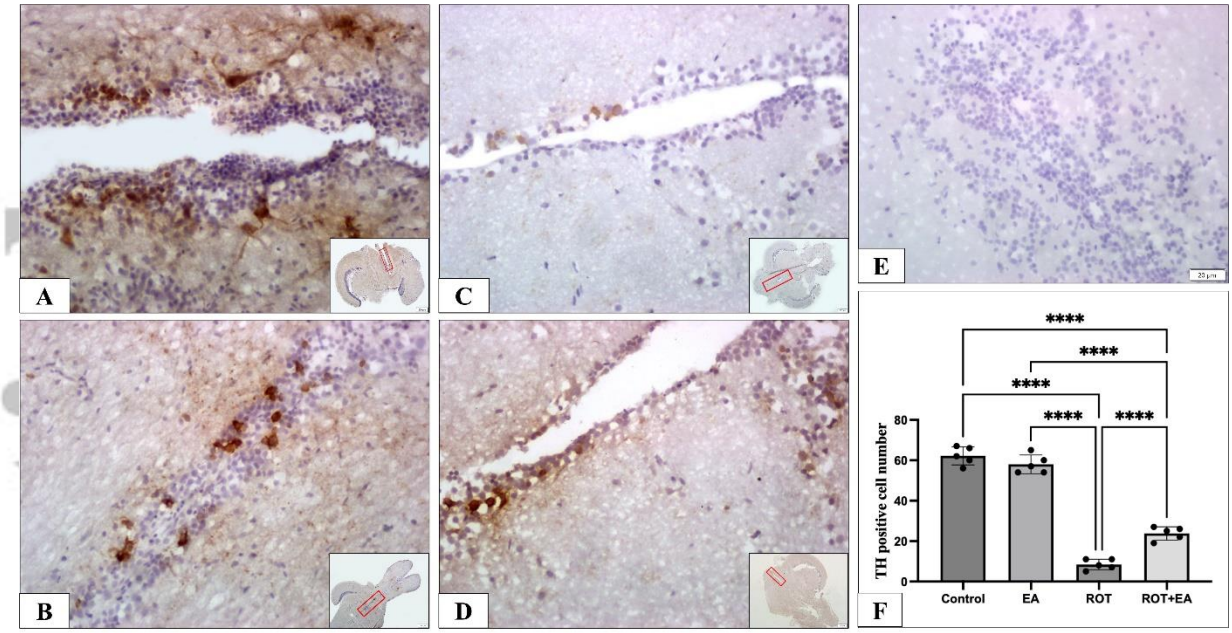

Figure 12: Photomicrographs of TH labeling dopaminergic neurons (brown color) in the brain regions in Control (A), EA (B), Rot (C), and Rot+EA (D) groups (n=5). Incubation with antibody diluent (without antibody) revealed no staining (E; negative control). The marked areas in the insets, given at an X4 magnification (bar: 200 µm) represent the original images. Original magnification X40 (bar: 20 µm). All images were captured the same adjustments. Graphic (F) shows TH positive cell number. **** p<0.0001, *** p<0.001, ** p<0.01, * p<0.05. EA: Erucic Acid Group; Rot:Rotenone Group; Rot+EA: Rotenone+Erucic Acid Group.

Graphical Abstract

LC-MS/MS analyzes showed 196 and 243 significantly dysregulated proteins in brain and intestines in the rotenone group. Erucic acid treatment improved locomotor activity, immunohistochemical TH expression, expressions of PD-related genes, and oxidant damage both in brain and intestines in the rotenone group.

Table 1: Forward and reverse primers used in the study.

park2	forward primer	5′GCGAGTGTGTCTGAGCTGAA-3′
	reverse primer	5′CACACTGGAACACCAGCACT-3′
pink1	forward primer	5′GGCAATGAAGATGATGTGGAAC-3′
	reverse primer	5′GGTCGGCAGGACATCAGGA-3′
lrrk2	forward primer	5′ -CCCTAAACCGCAGAGTATCA-3′
	reverse primer	5′ -ATTCATAGTCCACCGGTCTG-3′
park7	forward primer	50 -GGCCGGTAAAAGAGCGTTAG-30
	reverse primer	50 -ACCCATGAGTCCTCCACTA-30
β actin	forward primer	5′AAGCAGGAGTACGATGAGTCTG-3
	reverse primer	5′-GGTAAACGCTTCTGGAATGAC-3′

Table 2. Common proteins affected by rotenone and erucic acid treatments in brain tissues

Accession No	Gene Name	Description	Log2 Fold Change	Adj. p-Value
A0A0R4IXC8	Tubb6	Tubulin beta chain	4,54	0.000
A0A0R4IZ96	Neflb	Neurofilament light polypeptide	1,01	0.000
A0A1D5NS50	Hmgb3a	High mobility group box 3a	-1,25	0.002
A0A2R8Q9S7	Si:Dkey-46i9.1	Si:dkey-46i9.1	-1,25	0.002
A0A2R8QCR5	Slc35a4	Probable UDP-sugar transporter protein SLC35A4	1,74	0.000
A0A2R8QDV2	Cst14b.1	Cystatin 14b, tandem duplicate 1	1,18	0.006
A0A2R8QSU3	Calb2a	Calretinin	4,28	0.000
A5PLC8	Ptmab	Prothymosin alpha-B	-1,82	0.002
A5WWC6	Hsdl1	Inactive hydroxysteroid dehydrogenase-like protein 1	2,14	0.000
A8E5E5	Anxa3b	Annexin	-4,64	0.000
B2GRK9	Tktb	Tkt protein	-1,84	0.000
B8A615	Si:Dkey-33c12.3	Si:dkey-33c12.3	1,54	0.000
E9QD58	Mink1	Misshapen-like kinase 1	-1,36	0.000
E9QIE2	Omga	Oligodendrocyte myelin glycoprotein a (Fragment)	2,55	0.000
F1Q9Z2	Arl2	ADP-ribosylation factor-like 2	2,4	0.000
F1QCR7	Nefma	160 kDa neurofilament protein	1,7	0.000
F1QT60	Viml	Vimentin-like	1,38	0.000
F1RBU6	Aifm1	Apoptosis-inducing factor mitochondrion-associated 1	-2,32	0.000
F1RC67	Dgkh	Diacylglycerol kinase (Fragment)	-1,26	0.032
G4XPM3	Marcksb	Myristoylated alanine rich protein kinase C substrate b	-1,42	0.000
O42364	Apoeb	Apolipoprotein Eb	2,53	0.000
P62247	Rps8	40S ribosomal protein S8	-1,65	0.000
P87360	Inab	Gefiltin	-3,41	0.000
Q1L9H0	Cd9b	CD9 molecule b	1,7	0.018
Q4V8Z1	Tsnax	Zgc:114078	-1,41	0.042
Q5D018	Rbm8a	RNA-binding protein 8A	-3,23	0.000
Q5XJ73	Glipr2l	GLI pathogenesis-related 2,-like	-1,25	0.000
Q6DGD8	Rnpep	Arginyl aminopeptidase (Aminopeptidase B)	-2,2	0.002
Q6DHL6	Rps6	40S ribosomal protein S6	-1,01	0.019
Q6NZW8	Arl8ba	ADP-ribosylation factor-like protein 8B-A	-2,24	0.000
Q6P0S2	Vdac3	Voltage-dependent anion-selective channel protein 3	1,57	0.006
Q6TH48	Aldh2.2	Mitochondrial aldehyde dehydrogenase 2 family	1,68	0.001
Q7SXW9	Marcksb	Marcks protein (Fragment)	2,58	0.000
Q7T2T7	Mecp2	Methyl-CpG-binding protein 2	1,06	0.001
Q7ZUH8	Mgst3a	Microsomal glutathione S-transferase 3a	1,32	0.000
Q7ZUV8	Pebp1	Zgc:56033	1,05	0.022
Q90X19	Ckma	Creatine kinase	-1,3	0.000
R4GDQ0	Tpp2	Tripeptidyl-peptidase 2	1,91	0.006
Z4YIS0	Ppp1r12a	Protein phosphatase 1 regulatory subunit	3,95	0.000

Fold change (log2): abundance ratio between Rot+EA and Rot groups. The p-value adjusted using Benjamini-Hochberg correction for the false-discovery rate. All proteins in this list have been quantified with at least two peptides per protein.

Table 3. Common proteins affected by rotenone and erucic acid treatments in intestinal tissues

Accession No	Gene Name	Description	Log2 Fold Change	Adj. p-Value
E7FCP7	Gaa2	Si:ch73-12o23.1	-2,74	0.000
A0A2R8RK83	Pvalb9	Parvalbumin	-3,32	0.000
X1WHC2	Aimp2	Aminoacyl tRNA synthetase complex-interacting multifunctional protein 2 (Fragment)	-2,13	0.004
F1Q6E1	Hpda	4-hydroxyphenylpyruvate dioxygenase	4,31	0.000
A7MCF4	Ech1	Zgc:101710 protein (Fragment)	-4,33	0.000
Q566N7	Sqor	Sulfide quinone reductase-like (Yeast)	-4,23	0.000
Q860Y0	Si:Busm1-266f07.1	Novel MHC class II beta chain protein	-2,61	0.003
A0A0R4IGS2	Si:Ch73-55i23.1	Si:ch73-55i23.1	-2,83	0.000
Q7ZUS9	Etfa	Electron transfer flavoprotein subunit alpha	1,98	0.030
Q5U7N6	Tln1	Talin 1	3,69	0.000
F1R8Y3	Ifi44a6	Si:dkey-79f11.8 (Fragment)	2,09	0.018
F8W3L1	Acta2	Actin alpha 2, smooth muscle (Fragment)	2,72	0.000
Q6PBR5	Atp6v1g1	V-type proton ATPase subunit G	2,82	0.001
Q7ZUS4	Sult1st2	Cytosolic sulfotransferase 2	2,64	0.011
F1Q9D8	Bin2a	Bridging integrator 2a	2,64	0.001
F1QV15	Vtg6	Phosvitin (Fragment)	3,01	0.000
Q6NY97	Dao.2	D-amino-acid oxidase 2	-3,36	0.000
F1QJZ6	Tmod2	Tropomodulin 2	2,98	0.001
F1R9Y9	Etfb	Electron transfer flavoprotein subunit beta	2	0.027
Q08CF8	Mhc1uha	Zgc:153138	-3,43	0.000
A3KPR3	Histh1l1	Histone H1 like	2,09	0.017
Q5PNQ1	Si:Ch211-201h21.5	Novel protein containing an inosine-uridine preferring nucleoside hydrolase domain	4,52	0.000
Q6NWK3	Ranbp1	RAN-binding protein 1	1,97	0.012
Q4VBV2	Rps27.1	40S ribosomal protein S27	2,07	0.018
F1QD15	Ptgfrn	Prostaglandin F2 receptor inhibitor	-2,69	0.006
Q6NZS0	Cpa5	Cpa5 protein (Fragment)	3,44	0.000
B2GNX4	Glrx3	Glrx3 protein	2,78	0.000
Q8JI14	Rhcgl2	Ammonium transporter Rh type C-like 2	-3,71	0.000
Q642I9	Cox6a1	Cytochrome c oxidase subunit	3,32	0.000
F1RCK3	Si:Dkey-85k7.10	Si:dkey-85k7.10 (Fragment)	-2,17	0.004
A0A2R8Q9H0	Loc100002544	Endonuclease domain-containing 1 protein-like	-1,71	0.043
A0A140LH63	Si:Ch73-368j24.12	Si:ch73-368j24.12	1,77	0.036
A0A0G2L2U8	N/A	Ig-like domain-containing protein	2,72	0.009
F1QRX2	Sumo3b	Small ubiquitin-related modifier	4,23	0.000
Q6DEG5	Polr2eb	DNA-directed RNA polymerase II subunit E	2,7	0.007

N/A; not available. Fold change (log2): abundance ratio between Rot+EA and Rot groups. The p-value adjusted using Benjamini-Hochberg correction for the false-discovery rate. Accession number: UniprotKB AC/ID. All proteins in this list have been quantified with at least two peptides per protein.

Table 4. KEGG Pathway: Functional Enrichment Pathway by STRING

term ID	Description	Observed	Background	FDR	
dre01100	Metabolic pathways	36	1672	0.00047	Ak1, Hpda, Zgc:86599, Neu3.2, Pck1, Mthfd1b, Atp5d, Uap1l1, Npl, Atp6v1g1, Ca2, Umps, Cox6a1, Hsd17b4, Bcmo1b, Dao.2, Gatm, Mat2ab, Acaa2, Elovl6l, Uap1, Pgk1, Rpn1, NAGK, Atp5ib, Si:Ch211-195e19.1, SDSL, Uroc1, Si:Ch73-12o23.1, Cox5b2, Suclg2, Nme4, Sqrdl, Hibch, Aco2, LOC794381